

# Code Design for Radar STAP via Optimization Theory

Antonio De Maio, *Senior Member, IEEE*, Silvio De Nicola, *Student Member, IEEE*, Yongwei Huang, *Member, IEEE*, Daniel P. Palomar, *Senior Member, IEEE*, Shuzhong Zhang, and Alfonso Farina, *Fellow, IEEE*

**Abstract**—In this paper, we deal with the problem of constrained code optimization for radar space-time adaptive processing (STAP) in the presence of colored Gaussian disturbance. At the design stage, we devise a code design algorithm complying with the following optimality criterion: maximization of the detection performance under a control on the regions of achievable values for the temporal and spatial Doppler estimation accuracy, and on the degree of similarity with a pre-fixed radar code. The resulting quadratic optimization problem is solved resorting to a convex relaxation that belongs to the semidefinite program (SDP) class. An optimal solution of the initial problem is then constructed through a suitable rank-one decomposition of an optimal solution of the relaxed one. At the analysis stage, we assess the performance of the new algorithm both on simulated data and on the standard challenging the Knowledge-Aided Sensor Signal Processing and Expert Reasoning (KASSPER) datacube.

**Index Terms**—Nonconvex quadratic optimization, radar signal processing, semidefinite programming relaxation, space-time adaptive processing (STAP), waveform design.

## I. INTRODUCTION

**I**N recent years, various algorithms for radar signal design that rely heavily upon complicated processing and/or antenna architectures have been suggested. These techniques owe their genesis to several factors, including revolutionary technological advances (new flexible waveform generators, high speed signal processing hardware, digital array radar technology, etc.) and the stressing performance requirements, often imposed by defense applications in areas such as airborne early warning

and homeland security [1]. Increasingly complex operating scenarios call for sophisticated algorithms, with the ability to adapt and diversify dynamically the waveform to the operating environment in order to achieve a performance gain over classic radar waveforms [2], [3].

The synthesis of narrowband waveforms with a specified ambiguity function is considered in [4], [41]. The use of information theory to devise waveforms for the detection of extended radar targets is studied in [5]. The concept of matched-illumination for optimized target detection and identification has been the object of [6]–[9] (and references therein). Waveform optimization in the presence of colored disturbance with known covariance matrix is considered in [10] and [11]. Therein, the idea of optimized waveform under a similarity constraint is introduced. A different radar signal design approach, known as the radar coding, relies on the modulation of a pulse train parameters (amplitude, phase, and frequency) in order to synthesize waveforms with some specified properties. A substantial bulk of work is nowadays available in open literature about this topic [12]–[14].

In [15], focusing on the class of linearly coded pulse trains (both in amplitude and in phase), the authors propose a code selection algorithm which maximizes the detection performance but, at the same time, is capable of controlling both the region of achievable values for the Doppler estimation accuracy and the degree of similarity with a pre-fixed radar code. The conceived algorithm first relaxes the original problem into a convex one which belongs to the SDP class [16], [17]; then it derives an optimum code through a rank-one decomposition of an optimal solution of the relaxed problem.

Nevertheless, in several practical situations, the radar amplifiers usually work in saturation conditions and hence an amplitude modulation might be difficult (even if not impossible) to perform. To this end, in [18], the authors consider the synthesis of constant modulus phase coding schemes for radar coherent pulse trains. They study the cases of both continuous and finite phase alphabet, and formulate the code design in terms of a nonconvex, NP-hard, quadratic optimization problem. In order to approximate the optimal solutions, the authors propose techniques (with polynomial computational complexity) based on SDP relaxation and randomization.<sup>1</sup>

In this paper, we consider the problem of constrained code optimization for radar space-time adaptive processing (STAP) in the presence of colored Gaussian disturbance (including clutter,

Manuscript received April 08, 2009; accepted August 09, 2009. First published September 25, 2009; current version published January 13, 2010. The associate editor coordinating the review of this manuscript and approving it for publication was Prof. Amir Leshem. The work of A. De Maio and S. De Nicola is supported in part by the Regione Campania—VIDES Project, and by SELEX—Sistemi Integrati. The work of Y. Huang and D. P. Palomar is supported in part by the RPC07/08.EG23 project. The work of S. Zhang is supported in part by Hong Kong RGC Earmarked CUHK419208.

A. De Maio and S. De Nicola are with the Dipartimento di Ingegneria Biomedica, Elettronica e delle Telecomunicazioni, Università degli Studi di Napoli “Federico II,” I-80125 Napoli, Italy (e-mail: ademaio@unina.it; silviodenicola@gmail.com).

Y. Huang and D. P. Palomar are with the Department of Electronic and Computer Engineering, Hong Kong University of Science and Technology, Clear Water Bay, Kowloon, Hong Kong (e-mail: eeyw@ust.hk; palomar@ust.hk).

S. Zhang is with the Department of Systems Engineering and Engineering Management, The Chinese University of Hong Kong, Shatin, Hong Kong (e-mail: zhang@se.cuhk.edu.hk).

A. Farina is with SELEX—Sistemi Integrati, I-00131 Roma, Italy (e-mail: afarina@selex-si.com).

Color versions of one or more of the figures in this paper are available online at <http://ieeexplore.ieee.org>.

Digital Object Identifier 10.1109/TSP.2009.2032993

<sup>1</sup>SDP relaxation and randomization techniques [19] have also been used in other signal processing fields. For instance, in maximum likelihood multiuser detection [20], multiple input multiple output (MIMO) decoding [21], and transmit beamforming [22].

jamming, and thermal noise). The importance and the interest towards this problem stem from the observation that radar STAP has become very popular in the past few years. Nowadays, there are at least three excellent documents testifying the state of art in this research field: [23]–[25]. Furthermore, STAP with application to airborne moving target indication (MTI) radars has become a key topic of international conferences. Last but not least, radar STAP plays an important role in numerous civilian and military applications such as earth observation, surveillance, ground moving target indication (GMTI), reconnaissance, and others [24].

At the design stage, we adopt the classic STAP model of [23] and focus on transmitted signals belonging to the class of coded pulse trains. We propose a code selection algorithm which is optimum according to the following criterion: maximization of the detection performance under a control on the regions of achievable values for the temporal and spatial Doppler estimation accuracy, and on the degree of similarity with a pre-fixed radar code. Actually, this last constraint is equivalent to force a similarity between the ambiguity functions of the devised waveform and of the pulse train encoded with the pre-fixed sequence. The resulting optimization problem belongs to the family of non-convex quadratic programs [16], [17]. In order to solve it, we first resort to a relaxation of the original problem into a convex one that belongs to the semidefinite program (SDP) class. Then, the transmitted code is constructed through the rank-one decomposition techniques of [26], [27] and applied to an optimal solution of the relaxed problem. Remarkably, the entire code search algorithm entails a polynomial computational complexity.

At the analysis stage, we assess the performance of the new encoding algorithm in terms of detection performance, regions of estimation accuracies that estimators of the temporal and the spatial Doppler frequencies can theoretically achieve, and ambiguity function. The analysis is conducted both on simulated data and on the Knowledge-Aided Sensor Signal Processing and Expert Reasoning (KASSPER) [28] reference STAP datacube.

The results show that it is possible to tradeoff the aforementioned performance metrics. In other words, detection capabilities can be swapped for desirable properties of the waveform ambiguity function and/or for enlarged regions of achievable temporal/spatial Doppler estimation accuracies.

The paper is organized as follows. In Section II, we present the model for both the transmitted and the received coded signal; moreover we formulate the code design optimization problem. In Section III, we introduce the algorithm which exploits SDP relaxation and provides a solution to the aforementioned problem. In Section IV, we assess the performance of the proposed encoding method also in comparison with a standard radar code. Finally, in Section V, we draw conclusions and outline possible future research tracks.

### A. Notation

We adopt the notation of using boldface for vectors  $\mathbf{a}$  (lower case), and matrices  $\mathbf{A}$  (upper case).  $\mathbf{A}(n, m)$  is the  $(n, m)$ th entry of the matrix  $\mathbf{A}$ . The transpose operator and the conjugate transpose operator are denoted by the symbols  $(\cdot)^T$  and  $(\cdot)^\dagger$ , respectively.  $\text{tr}(\cdot)$  is the trace of the square matrix argument,  $\mathbf{I}$

and  $\mathbf{O}$  denote, respectively, the identity matrix and the matrix with zero entries, while  $\mathbf{e}_k$  is the vector with all zeros except 1 in the  $k$ th position (their size is determined from the context). The letter  $j$  represents the imaginary unit (i.e.,  $j = \sqrt{-1}$ ), while the letter  $i$  often serves as index in this paper. For any complex number  $x$ , we use  $\Re(x)$  and  $\Im(x)$  to denote respectively the real and the imaginary parts of  $x$ ,  $|x|$  and  $\arg(x)$  represent the modulus and the argument of  $x$ , and  $x^*$  stands for the conjugate of  $x$ . The Euclidean norm of the vector  $\mathbf{x}$  is denoted by  $\|\mathbf{x}\|$ . The symbols  $\odot$  and  $\otimes$  represent the Hadamard element-wise and the Kronecker product, respectively [29]. The curled inequality symbol  $\succeq$  (and its strict form  $\succ$ ) is used to denote generalized inequality:  $\mathbf{A} \succeq \mathbf{B}$  means that  $\mathbf{A} - \mathbf{B}$  is an Hermitian positive semidefinite matrix ( $\mathbf{A} \succ \mathbf{B}$  for positive definiteness).

## II. SYSTEM MODEL AND PROBLEM FORMULATION

The STAP signal model adopted in this paper is that developed in [23, ch. 1], with the addition of a temporal coding on the transmitted coherent burst of pulses. Specifically, data are collected by a narrowband antenna array with  $M$  spatial channels which, for simplicity, we assume colinear, omnidirectional, and equally spaced. Each channel receives  $N$  echoes corresponding to the returns of a coherent coded pulse train composed of  $N$  pulses. It is assumed that the complex envelope of the transmitted signal is

$$u(t) = a_t e^{j\Phi_t} \sum_{i=0}^{N-1} c(i) p(t - iT_r)$$

where  $T_r$  is the pulse repetition time (PRT),  $[c(0), c(1), \dots, c(N-1)]^T = \mathbf{c} \in \mathbb{C}^N$  is the radar code (assumed without loss of generality with unit norm),  $p(t)$  is the pulse waveform of duration  $T_p$  and with unit energy,  $a_t$  and  $\Phi_t$  are respectively the amplitude and the random phase of  $u(t)$ .

Following [23], we formulate the problem of detecting a target in the presence of observables in terms of the following binary hypothesis test:

$$\begin{cases} H_0 : \mathbf{r} = \mathbf{i} + \mathbf{n} \\ H_1 : \mathbf{r} = \alpha \mathbf{p} + \mathbf{i} + \mathbf{n} \end{cases} \quad (1)$$

where  $\mathbf{r}$  is the  $MN \times 1$  *space-time snapshot* at the range of interest,  $\mathbf{i}$  and  $\mathbf{n}$  denote respectively the clutter/interference and receiver noise vectors which are assumed statistically independent zero-mean complex circular Gaussian vectors,  $\alpha$  is the complex amplitude accounting for both the target as well as the channel propagation effects, and  $\mathbf{p}$  the target *space-time steering vector*, i.e.,  $\mathbf{p} = (\mathbf{c} \odot \mathbf{p}_t) \otimes \mathbf{p}_s$ , with  $\mathbf{p}_t$  ( $N$ -dimensional) and  $\mathbf{p}_s$  ( $M$ -dimensional) being respectively the temporal and the spatial steering vectors. More precisely [23],  $\mathbf{p}_t = (1/\sqrt{N})[1, \exp(j2\pi f_t), \dots, \exp(j2\pi(N-1)f_t)]^T$ ,  $\mathbf{p}_s = (1/\sqrt{M})[1, \exp(j2\pi f_s), \dots, \exp(j2\pi(M-1)f_s)]^T$ , with  $f_t$  and  $f_s$  the normalized temporal and spatial Doppler frequencies, respectively.

A common measure of a STAP processor performance is the output signal-to-interference-plus-noise ratio (SINR) [23, pp. 62-69], which, for the optimum filter, is given by

$$\text{SINR} = |\alpha|^2 [(\mathbf{c} \odot \mathbf{p}_t) \otimes \mathbf{p}_s]^\dagger \mathbf{M} [(\mathbf{c} \odot \mathbf{p}_t) \otimes \mathbf{p}_s] \quad (2)$$

where  $\mathbf{M} = \mathbf{R}_{\mathbf{i}, \mathbf{n}}^{-1} \succ 0$  and  $\mathbf{R}_{\mathbf{i}, \mathbf{n}} = E[(\mathbf{i} + \mathbf{n})(\mathbf{i} + \mathbf{n})^\dagger]$  ( $E[\cdot]$  denotes statistical expectation) is the  $MN \times MN$ -dimensional disturbance space-time covariance matrix (due to clutter/interference and thermal noise). Indeed, due to the Gaussian assumption, maximizing the SINR is tantamount to maximizing the detection performance. The following lemma will be useful in simplifying some of the subsequent expressions and derivations.

*Lemma 1:* Let  $\mathbf{M} \in \mathbb{C}^{MN \times MN}$  be a Hermitian matrix,  $\mathbf{a} \in \mathbb{C}^N$ ,  $\mathbf{b} \in \mathbb{C}^M$ . Then,

$$[(\mathbf{c} \odot \mathbf{a}) \otimes \mathbf{b}]^\dagger \mathbf{M} [(\mathbf{c} \odot \mathbf{a}) \otimes \mathbf{b}] = \mathbf{c}^\dagger \mathbf{R} \mathbf{c} \quad (3)$$

where the  $N \times N$  Hermitian matrix  $\mathbf{R}$  is given by

$$\mathbf{R} = [(\mathbf{I} \otimes \mathbf{b})^\dagger \mathbf{M} (\mathbf{I} \otimes \mathbf{b})] \odot (\mathbf{a} \mathbf{a}^\dagger)^*. \quad (4)$$

Furthermore, 1) if  $\mathbf{M}$  is positive semidefinite, then  $\mathbf{R}$  is positive semidefinite, 2) if  $\mathbf{M}$  is positive definite, all the entries of  $\mathbf{a}$  are nonzero, and  $\mathbf{b} \neq \mathbf{0}$ , then  $\mathbf{R}$  is positive definite, and 3) if  $\mathbf{M}$  is positive definite, and  $\mathbf{a}$  has at least a zero entry, then  $\mathbf{R}$  is positive semidefinite.

*Proof:* See Appendix A.

The goal of this paper is to design the code  $\mathbf{c}$  that maximizes the output SINR (2), under some constraints that allow controlling the region of achievable temporal and spatial Doppler estimation accuracies and force a similarity with a given radar code  $\mathbf{c}_0$  (assumed with unit norm). This last constraint is necessary in order to control the ambiguity function of the transmitted coded pulse train (as  $\mathbf{c}_0$  has a good ambiguity function); it can be formalized as  $\|\mathbf{c} - \mathbf{c}_0\|^2 \leq \epsilon$ , where the parameter  $\epsilon$  (with  $0 < \epsilon < 2$  for unit norm vectors  $\mathbf{c}$  and  $\mathbf{c}_0$ ) rules the size of the similarity region<sup>2</sup> [15, Sec. III C].

Concerning the region of achievable temporal and spatial Doppler estimation, the most natural choice would be forcing upper bounds on the Cramér–Rao bounds (CRBs) on  $f_t$  and  $f_s$  for known  $\alpha$  and unknown temporal and spatial Doppler frequencies. Unfortunately, this approach leads to intractable nonconvex constraints. However, this drawback can be circumvented constraining the CRB on  $f_t$  for known  $\alpha$  and  $f_s$ , and the CRB on  $f_s$  for known  $\alpha$  and  $f_t$ . As we will see, this formulation still leads to nonconvex constraints which, despite the previous case, are quadratic. Further developments require specifying the following:

- the CRB, for known  $\alpha$  and  $f_s$ , with respect to the estimation of  $f_t$  is given by [30, Sec. 8.2.3.1]

$$\Delta_{\text{CR}}(f_t) = \Psi \left\{ \left[ \left( \mathbf{c} \odot \frac{\partial \mathbf{p}_t}{\partial f_t} \right) \otimes \mathbf{p}_s \right]^\dagger \mathbf{M} \times \left[ \left( \mathbf{c} \odot \frac{\partial \mathbf{p}_t}{\partial f_t} \right) \otimes \mathbf{p}_s \right] \right\}^{-1} \quad (5)$$

with  $\Psi = 1/2|\alpha|^2$ ;

- the CRB, for known  $\alpha$  and  $f_t$ , with respect to the estimation of  $f_s$  is given by

$$\Delta_{\text{CR}}(f_s) = \Psi \left\{ \left[ \left( \mathbf{c} \odot \mathbf{p}_t \right) \otimes \frac{\partial \mathbf{p}_s}{\partial f_s} \right]^\dagger \mathbf{M} \left[ \left( \mathbf{c} \odot \mathbf{p}_t \right) \otimes \frac{\partial \mathbf{p}_s}{\partial f_s} \right] \right\}^{-1}. \quad (6)$$

<sup>2</sup>If  $\epsilon = 2$ , the similarity constraint vanishes; in practice, this  $\epsilon$  is quite small.

As to the regions of achievable temporal and spatial Doppler estimation accuracies (denoted as  $\mathcal{A}_t$  and  $\mathcal{A}_s$ , respectively), they can be controlled forcing upper bounds on the respective CRBs (see [15, Sec. III B] for a discussion in the case of temporal processing only and for a pictorial description). To this end, forcing upper bounds to (5) and (6), for a specified  $\Psi$  value, results in lower bounds on the sizes of  $\mathcal{A}_t$  and  $\mathcal{A}_s$ . Hence, according to this guideline, we focus on radar codes complying with

$$\Delta_{\text{CR}}(f_t) \leq \frac{\Psi}{\delta_t} \quad \text{and} \quad \Delta_{\text{CR}}(f_s) \leq \frac{\Psi}{\delta_s} \quad (7)$$

or equivalently

$$\left[ \left( \mathbf{c} \odot \frac{\partial \mathbf{p}_t}{\partial f_t} \right) \otimes \mathbf{p}_s \right]^\dagger \mathbf{M} \left[ \left( \mathbf{c} \odot \frac{\partial \mathbf{p}_t}{\partial f_t} \right) \otimes \mathbf{p}_s \right] \geq \delta_t \quad (8)$$

$$\left[ \left( \mathbf{c} \odot \mathbf{p}_t \right) \otimes \frac{\partial \mathbf{p}_s}{\partial f_s} \right]^\dagger \mathbf{M} \left[ \left( \mathbf{c} \odot \mathbf{p}_t \right) \otimes \frac{\partial \mathbf{p}_s}{\partial f_s} \right] \geq \delta_s \quad (9)$$

where  $\delta_t$  and  $\delta_s$  are two positive real numbers ruling the upper bounds on CRBs.

Exploiting Lemma I, the SINR in (2) and the left-hand side (LHS) of (8) and (9) can be rewritten as

$$\begin{aligned} \left[ \left( \mathbf{c} \odot \mathbf{p}_t \right) \otimes \mathbf{p}_s \right]^\dagger \mathbf{M} \left[ \left( \mathbf{c} \odot \mathbf{p}_t \right) \otimes \mathbf{p}_s \right] &= \mathbf{c}^\dagger \mathbf{R} \mathbf{c} \\ \left[ \left( \mathbf{c} \odot \frac{\partial \mathbf{p}_t}{\partial f_t} \right) \otimes \mathbf{p}_s \right]^\dagger \mathbf{M} \left[ \left( \mathbf{c} \odot \frac{\partial \mathbf{p}_t}{\partial f_t} \right) \otimes \mathbf{p}_s \right] &= \mathbf{c}^\dagger \mathbf{R}_t \mathbf{c} \\ \left[ \left( \mathbf{c} \odot \mathbf{p}_t \right) \otimes \frac{\partial \mathbf{p}_s}{\partial f_s} \right]^\dagger \mathbf{M} \left[ \left( \mathbf{c} \odot \mathbf{p}_t \right) \otimes \frac{\partial \mathbf{p}_s}{\partial f_s} \right] &= \mathbf{c}^\dagger \mathbf{R}_s \mathbf{c} \end{aligned}$$

where  $\mathbf{R} = [(\mathbf{I} \otimes \mathbf{p}_s)^\dagger \mathbf{M} (\mathbf{I} \otimes \mathbf{p}_s)] \odot (\mathbf{p}_t \mathbf{p}_t^\dagger)^* \succ \mathbf{0}$ ,  $\mathbf{R}_t = [(\mathbf{I} \otimes \mathbf{p}_s)^\dagger \mathbf{M} (\mathbf{I} \otimes \mathbf{p}_s)] \odot ((\partial \mathbf{p}_t / \partial f_t) (\partial \mathbf{p}_t / \partial f_t)^\dagger)^* \succeq \mathbf{0}$  (because the first component of  $\partial \mathbf{p}_t / \partial f_t$  is zero), and  $\mathbf{R}_s = [(\mathbf{I} \otimes (\partial \mathbf{p}_s / \partial f_s))^\dagger \mathbf{M} (\mathbf{I} \otimes (\partial \mathbf{p}_s / \partial f_s))] \odot (\mathbf{p}_t \mathbf{p}_t^\dagger)^* \succ \mathbf{0}$ .

It follows that the problem of devising the STAP code, under (8) and (9), the similarity and the energy constraints, can be formulated as the following nonconvex quadratic optimization problem (QP):

$$\text{QP} \begin{cases} \text{maximize}_{\mathbf{c}} & \mathbf{c}^\dagger \mathbf{R} \mathbf{c} \\ \text{subject to} & \mathbf{c}^\dagger \mathbf{c} = 1 \\ & \mathbf{c}^\dagger \mathbf{R}_t \mathbf{c} \geq \delta_t \\ & \mathbf{c}^\dagger \mathbf{R}_s \mathbf{c} \geq \delta_s \\ & \|\mathbf{c} - \mathbf{c}_0\|^2 \leq \epsilon \end{cases} \quad (10)$$

which can be equivalently written as

$$\text{QP} \begin{cases} \text{maximize}_{\mathbf{c}} & \mathbf{c}^\dagger \mathbf{R} \mathbf{c} \\ \text{subject to} & \mathbf{c}^\dagger \mathbf{c} = 1 \\ & \mathbf{c}^\dagger \mathbf{R}_t \mathbf{c} \geq \delta_t \\ & \mathbf{c}^\dagger \mathbf{R}_s \mathbf{c} \geq \delta_s \\ & \Re(\mathbf{c}^\dagger \mathbf{c}_0) \geq 1 - \epsilon/2. \end{cases}$$

Evidently, problem (10) requires the specification of  $f_t$  and  $f_s$ ; as a consequence, the solution code depends on these pre-assigned values. It is thus necessary to provide some guidelines on the importance and the applicability of the proposed framework. To this end, we highlight the following.

- The performance level which can be obtained through the optimal solution of (10), in correspondence of the design

$f_t$  and  $f_s$ , represents an upper bound to that achievable by any practically implementable system.

- The encoding procedure might be applied in a waveform diversity context, where more coded waveforms on different carriers are transmitted [31]. These waveforms are chosen frequency orthogonal and each of them is optimized for the detection in a given spatial-temporal frequency bin. At the receiver end, the detector tuned to the specific bin processes its matched waveform [32].
- A single coded waveform designed for the challenging condition of slowly moving target close to the clutter ridge [23] can be transmitted.
- A single coded waveform optimized to an average scenario can be selected. Otherwise stated, the code might be chosen as the solution to the problem (10) with  $\mathbf{R}$ ,  $\mathbf{R}_t$ , and  $\mathbf{R}_s$  replaced by  $E[\mathbf{R}]$ ,  $E[\mathbf{R}_t]$ , and  $E[\mathbf{R}_s]$ , where the expectation operator is over  $f_t$  and  $f_s$ . If these last quantities are modeled as independent random variables, the expectations can be evaluated after some algebra, i.e.,  $E[\mathbf{R}(h, k)] = \text{tr}[\mathbf{M} \odot (\mathbf{e}_h \mathbf{e}_k^T \otimes \mathbf{B})] \mathbf{A}(h, k)$ ,  $E[\mathbf{R}_t(h, k)] = 4\pi^2 h k \text{tr}[\mathbf{M} \odot (\mathbf{e}_h \mathbf{e}_k^T \otimes \mathbf{B})] \mathbf{A}(h, k)$ ,  $E[\mathbf{R}_s(h, k)] = 4\pi^2 \text{tr}\{\mathbf{M} \odot [\mathbf{e}_h \mathbf{e}_k^T \otimes (\mathbf{B} \odot \mathbf{U})]\} \mathbf{A}(h, k)$ , where  $\mathbf{B} = E[\mathbf{p}_s \mathbf{p}_s^\dagger]$  and  $\mathbf{A} = E[\mathbf{p}_t \mathbf{p}_t^\dagger]$ , while  $\mathbf{U}$  is the  $M \times M$  matrix with entries  $\mathbf{U}(m, n) = mn$ . In particular, if  $f_t$  and  $f_s$  are modeled as independent random variables uniformly distributed in  $(-\Delta_t, \Delta_t)$  and  $(-\Delta_s, \Delta_s)$ , respectively, we have  $\mathbf{B}(h, k) = (1/M) \text{sinc}(2\Delta_s(h - k))$ ,  $\mathbf{A}(h, k) = (1/N) \text{sinc}(2\Delta_t(h - k))$ , with the sinc( $\cdot$ ) function defined as  $\text{sinc}(x) = \sin(\pi x)/\pi x$ .
- Assume that, after an uncoded (or a possibly standard coded) transmission, a detection is declared in a given spatial-temporal Doppler bin. Our coding procedure can be thus employed to shape the waveform for the next transmission in order to confirm the detection in the previously identified bin.

### III. SOLUTION TO THE OPTIMIZATION PROBLEM

In this section, we demonstrate how to obtain an optimal solution of QP. Toward this, we consider the following enlarged quadratic problem (EQP):

$$\text{EQP} \begin{cases} \underset{\mathbf{c}}{\text{maximize}} & \mathbf{c}^\dagger \mathbf{R} \mathbf{c} \\ \text{subject to} & \mathbf{c}^\dagger \mathbf{c} = 1 \\ & \mathbf{c}^\dagger \mathbf{R}_t \mathbf{c} \geq \delta_t \\ & \mathbf{c}^\dagger \mathbf{R}_s \mathbf{c} \geq \delta_s \\ & \Re^2(\mathbf{c}^\dagger \mathbf{c}_0) + \Im^2(\mathbf{c}^\dagger \mathbf{c}_0) = \mathbf{c}^\dagger \mathbf{c}_0 \mathbf{c}_0^\dagger \mathbf{c} \geq \delta_\epsilon \end{cases} \quad (11)$$

where  $\delta_\epsilon = (1 - \epsilon/2)^2$ , and claim the following lemma:

*Lemma II:* Let  $\bar{\mathbf{c}}$  be an optimal solution of EQP. Then, the solution  $\bar{\mathbf{c}} e^{j \arg(\bar{\mathbf{c}}^\dagger \mathbf{c}_0)}$  is optimal to QP.

*Proof:* See Appendix B.

This implies that we can construct an optimal solution of QP from an optimal solution of EQP, and the problems QP and EQP possess the same optimal value. Now, we are going to find an

optimal solution of EQP. To this end, we exploit the equivalent matrix formulation

$$\text{EQP} \begin{cases} \underset{\mathbf{C}}{\text{maximize}} & \text{tr}(\mathbf{C} \mathbf{R}) \\ \text{subject to} & \text{tr}(\mathbf{C}) = 1 \\ & \text{tr}(\mathbf{C} \mathbf{R}_t) \geq \delta_t \\ & \text{tr}(\mathbf{C} \mathbf{R}_s) \geq \delta_s \\ & \text{tr}(\mathbf{C} \mathbf{C}_0) \geq \delta_\epsilon \\ & \mathbf{C} = \mathbf{c} \mathbf{c}^\dagger \end{cases} \quad (12)$$

where  $\mathbf{C}_0 = \mathbf{c}_0 \mathbf{c}_0^\dagger$ .

Problem (12) can be relaxed into an SDP<sup>3</sup> problem neglecting the rank-one constraint [19]. By doing so, we obtain a relaxed enlarged quadratic problem (REQP)

$$\text{REQP} \begin{cases} \underset{\mathbf{C}}{\text{maximize}} & \text{tr}(\mathbf{C} \mathbf{R}) \\ \text{subject to} & \text{tr}(\mathbf{C}) = 1 \\ & \text{tr}(\mathbf{C} \mathbf{R}_t) \geq \delta_t \\ & \text{tr}(\mathbf{C} \mathbf{R}_s) \geq \delta_s \\ & \text{tr}(\mathbf{C} \mathbf{C}_0) \geq \delta_\epsilon \\ & \mathbf{C} \succeq \mathbf{0}. \end{cases} \quad (13)$$

The dual problem of REQP, REQPD, is

$$\text{REQPD} \begin{cases} \underset{y_1, y_2, y_3, y_4}{\text{minimize}} & y_1 - y_2 \delta_t - y_3 \delta_s - y_4 \delta_\epsilon \\ \text{subject to} & y_1 \mathbf{I} - y_2 \mathbf{R}_t - y_3 \mathbf{R}_s - y_4 \mathbf{C}_0 \succeq \mathbf{R} \\ & y_2 \geq 0, y_3 \geq 0, y_4 \geq 0. \end{cases}$$

Throughout the paper, we assume that QP is strictly feasible, namely there is  $\mathbf{c}_1$  such that  $\|\mathbf{c}_1\| = 1$ ,  $\mathbf{c}_1^\dagger \mathbf{R}_t \mathbf{c}_1 > \delta_t$ ,  $\mathbf{c}_1^\dagger \mathbf{R}_s \mathbf{c}_1 > \delta_s$ , and  $\Re(\mathbf{c}_1^\dagger \mathbf{c}_0) > 1 - \epsilon/2$  (to this end, it is sufficient to suppose that the initial code  $\mathbf{c}_0$  is a strictly feasible solution of QP). We claim that both REQP and REQPD are strictly feasible.<sup>4</sup> It follows, by the weak duality theorem, that REQP is bounded above and REQPD is bounded below. Also, it follows, by the strong duality theorem of SDP (for example, see [17, Theorem 1.7.1]), that the optimal values of REQP and REQPD are equal and attainable at some optimal points. Moreover, the complementary slackness conditions are satisfied at the optimal points of the primal and the dual problems. Denote by  $v(\cdot)$  the optimal value of the problem ( $\cdot$ ). It is known from optimization theory that REQPD is also the dual problem of EQP. So far, we have established the following relationships:

$$\begin{aligned} v(\text{REQP}) &= v(\text{REQPD}) \\ &\quad (\text{from strong duality theorem of SDP}) \\ &\geq v(\text{EQP}) \quad (\text{from the weak duality theorem}) \\ &= v(\text{QP}) \quad (\text{from Lemma II}). \end{aligned}$$

As a consequence, solving the SDP problem REQP provides an upper bound to EQP (or the original problem QP). Furthermore, as long as we can get a rank-one optimal solution of REQP in

<sup>3</sup>An SDP is a convex optimization problem that can be efficiently solved in polynomial time through *interior point methods* [16], namely iterative algorithms which terminate once a pre-specified accuracy  $\zeta$  is reached. The number of iterations necessary to achieve convergence usually ranges between 10 and 100 [16].

<sup>4</sup>Further details on the strict feasibility of REQP and REQPD are given in Appendix C.

some way, the upper bound is tight; in other words, the SDP relaxation of EQP is exact, or equivalently, strong duality for the nonconvex problem EQP holds (i.e.,  $v(\text{REQPD}) = v(\text{EQP})$ ). Therefore, to solve EQP (or QP), it suffices for us to find a rank-one optimal solution of the SDP problem, which is our focus in the remainder of the paper.

Before proceeding, let us compare the optimization problem solved in [15] with that we are faced with in the present paper. In [15], the authors show strong duality for the following problem:

$$\begin{cases} \underset{\mathbf{C}}{\text{maximize}} & \text{tr}(\mathbf{C}\mathbf{R}) \\ \text{subject to} & \text{tr}(\mathbf{C}) = 1 \\ & \text{tr}(\mathbf{C}\mathbf{R}_t) \geq \delta_t \\ & \text{tr}(\mathbf{C}\mathbf{C}_0) \geq \delta_\epsilon \\ & \mathbf{C} = \mathbf{c}\mathbf{c}^\dagger \end{cases} \quad (14)$$

and find an optimal solution of (14), resorting to the SDP relaxation technique and the special rank-one decomposition procedure of [26]; in other words, (14) has been proven to be a *hidden* convex program. The most significant difference between (14) and (12) (i.e., EQP) is that the former includes only three homogeneous quadratic constraints, while the latter has four. As a consequence, strong duality for problem EQP may or may not hold. In what follows, we identify most cases where the strong duality is valid, and propose solution procedures, resorting to either the rank-one decomposition theorem of [26], or the new rank-one decomposition proposed in [27]. We explicitly highlight that the techniques used in this paper are far trickier and more involved than those exploited in [15].

The analysis of the relaxed problem REQPD and its dual REQPD is easy as REQPD is a convex problem. Indeed, denote by  $\bar{\mathbf{C}}$  an optimal solution of REQPD, and by  $(\bar{y}_1, \bar{y}_2, \bar{y}_3, \bar{y}_4)$  an optimal solution of REQPD. Then, the primal-dual optimal solution pair  $(\bar{\mathbf{C}}, \bar{y}_1, \bar{y}_2, \bar{y}_3, \bar{y}_4)$  satisfies the Karush–Kuhn–Tucker optimality conditions (which are sufficient and necessary, since SDP is a convex optimization problem and constraint qualification conditions (Slater's conditions [16]) are satisfied). In particular, the complementary slackness conditions are

$$\text{tr}[(\bar{y}_1\mathbf{I} - \bar{y}_2\mathbf{R}_t - \bar{y}_3\mathbf{R}_s - \bar{y}_4\mathbf{C}_0 - \mathbf{R})\bar{\mathbf{C}}] = 0 \quad (15)$$

$$(\text{tr}(\bar{\mathbf{C}}\mathbf{R}_t) - \delta_t)\bar{y}_2 = 0 \quad (16)$$

$$(\text{tr}(\bar{\mathbf{C}}\mathbf{R}_s) - \delta_s)\bar{y}_3 = 0 \quad (17)$$

$$(\text{tr}(\bar{\mathbf{C}}\mathbf{C}_0) - \delta_\epsilon)\bar{y}_4 = 0. \quad (18)$$

Further developments require the following rank-one decomposition theorems which have been proved in [26] and [27], respectively.

**Proposition I:** Suppose that  $\mathbf{X}$  is an  $N \times N$  complex Hermitian positive semidefinite matrix of rank  $R$ , and  $\mathbf{A}_1, \mathbf{A}_2$  are two  $N \times N$  given Hermitian matrices. Then, there is a rank-one decomposition of  $\mathbf{X}$  (synthetically denoted as  $\mathcal{D}_2(\mathbf{X}, \mathbf{A}_1, \mathbf{A}_2)$ ),

$$\mathbf{X} = \sum_{r=1}^R \mathbf{x}_r \mathbf{x}_r^\dagger \quad (19)$$

such that

$$\mathbf{x}_r^\dagger \mathbf{A}_1 \mathbf{x}_r = \frac{\text{tr}(\mathbf{X}\mathbf{A}_1)}{R} \quad \text{and} \quad \mathbf{x}_r^\dagger \mathbf{A}_2 \mathbf{x}_r = \frac{\text{tr}(\mathbf{X}\mathbf{A}_2)}{R}. \quad (20)$$

*Proof:* See [26, Theorem 2.1].

**Proposition II:** Let  $\mathbf{X}$  be a nonzero  $N \times N$  ( $N \geq 3$ ) complex Hermitian positive semidefinite matrix, and suppose that  $(\text{tr}(\mathbf{Y}\mathbf{A}_1), \text{tr}(\mathbf{Y}\mathbf{A}_2), \text{tr}(\mathbf{Y}\mathbf{A}_3), \text{tr}(\mathbf{Y}\mathbf{A}_4)) \neq (0, 0, 0, 0)$  for any nonzero complex Hermitian positive semidefinite matrix  $\mathbf{Y}$  of size  $N \times N$ . Then,

- if  $\text{rank}(\mathbf{X}) \geq 3$ , one can find, in polynomial time, a rank-one matrix  $\mathbf{x}\mathbf{x}^\dagger$  such that  $\mathbf{x}$  (synthetically denoted as  $\mathcal{D}_4(\mathbf{X}, \mathbf{A}_1, \mathbf{A}_2, \mathbf{A}_3, \mathbf{A}_4)$ ) is in  $\text{range}(\mathbf{X})$ , and

$$\mathbf{x}^\dagger \mathbf{A}_i \mathbf{x} = \text{tr}(\mathbf{X}\mathbf{A}_i), \quad i = 1, 2, 3, 4;$$

- if  $\text{rank}(\mathbf{X}) = 2$ , for any  $\mathbf{z}$  not in the range space of  $\mathbf{X}$ , one can find a rank-one matrix  $\mathbf{x}\mathbf{x}^\dagger$  such that  $\mathbf{x}$  is in the linear subspace spanned by  $\{\mathbf{z}\} \cup \text{range}(\mathbf{X})$ , and

$$\mathbf{x}^\dagger \mathbf{A}_i \mathbf{x} = \text{tr}(\mathbf{X}\mathbf{A}_i), \quad i = 1, 2, 3, 4.$$

*Proof:* See [27, Theorem 2.3].

The computational complexity of each rank-one decomposition theorem requires  $O(N^3)$  [26], [27]. In fact, the computation involves both a Cholesky factorization and suitable rotations. Hence, the required amount of operations is dominated by that necessary for the Cholesky decomposition, which is known to be  $O(N^3)$ .

As already pointed out, once a rank-one positive semidefinite matrix  $\mathbf{C}$  satisfying (15)–(18) and feasible to (13) has been found, we can claim that  $\mathbf{C} = \mathbf{c}\mathbf{c}^\dagger$  is an optimal solution of (12), or equivalently,  $\mathbf{c}$  is an optimal solution of (11). Now, we aim at finding a procedure to construct a rank-one optimal solution of REQPD from a general rank optimal solution  $\bar{\mathbf{C}}$  of REQPD, which can always be found by an SDP solver. We claim the following two main theorems.

**Theorem I:** Let  $\bar{\mathbf{C}}$  be an optimal solution of REQPD with  $\text{rank}(\bar{\mathbf{C}}) \geq 3$ . Then, we can find a rank-one optimal solution of REQPD in polynomial time.

*Proof:* See Appendix D.

**Theorem II:** Let  $\bar{\mathbf{C}}$  be an optimal solution of REQPD with  $\text{rank}(\bar{\mathbf{C}}) = 2$ . Then, if one of the inequalities is satisfied:  $\text{tr}(\bar{\mathbf{C}}\mathbf{R}_t) > \delta_t$ ,  $\text{tr}(\bar{\mathbf{C}}\mathbf{R}_s) > \delta_s$ , or  $\text{tr}(\bar{\mathbf{C}}\mathbf{C}_0) > \delta_\epsilon$ , we can find a rank-one optimal solution of REQPD in polynomial time.

*Proof:* See Appendix E.

We remark that in Theorem I, the assumption  $\text{rank}(\bar{\mathbf{C}}) \geq 3$  implies that the size  $N$  of  $\bar{\mathbf{C}}$  is greater than or equal to 3, i.e., the length of radar code is not smaller than 3, which is practical. Note that in Theorem II, the size  $N$  of  $\bar{\mathbf{C}}$  could be greater than or equal to 2.

Also, from the proofs, we can deduce the construction procedure of a rank-one optimal solution of EQP. Actually, the solution procedure for (12) based on the above two theorems is very different from the solution procedure for (14), introduced in [15] through the application of Proposition I to any optimal solution  $\bar{\mathbf{C}}$  with rank higher than one.

In the following, we summarize the procedure that leads to an optimal solution of EQP, by distinguishing among three possible cases.

**Case 1:**  $\text{rank}(\bar{\mathbf{C}}) = 1$ . In this case, a vector  $\mathbf{c}$  with  $\bar{\mathbf{C}} = \mathbf{c}\mathbf{c}^\dagger$  is an optimal solution of EQP.

**Case 2:**  $\text{rank}(\bar{\mathbf{C}}) \geq 3$ . Exploiting Theorem I, we can obtain a rank-one optimal solution of REQP.

**Case 3:**  $\text{rank}(\bar{\mathbf{C}}) = 2$ . Let  $\text{tr}(\bar{\mathbf{C}}\mathbf{R}_t) = \delta_2$ ,  $\text{tr}(\bar{\mathbf{C}}\mathbf{R}_s) = \delta_3$  and  $\text{tr}(\bar{\mathbf{C}}\mathbf{C}_0) = \delta_4$ . We have to consider two possible situations:

**Case 3.1:** One of the inequalities  $\delta_2 > \delta_t$ ,  $\delta_3 > \delta_s$ , or  $\delta_4 > \delta_\epsilon$  holds. In this case, we invoke Theorem II to output a rank-one optimal solution of REQP.

**Case 3.2:**  $\delta_2 = \delta_t$ ,  $\delta_3 = \delta_s$ ,  $\delta_4 = \delta_\epsilon$ . In this case, we are not able to judge whether the strong duality is valid for (13). Nevertheless, we can still provide a procedure aimed at constructing feasible solutions for (13). Precisely, according to the last claim of Proposition II, for any vector  $\mathbf{z} \notin \text{range}(\bar{\mathbf{C}})$ , we can obtain a vector  $\mathbf{c}_z$  such that

$$\begin{aligned} \text{tr}(\mathbf{c}_z \mathbf{c}_z^\dagger) &= \text{tr}(\bar{\mathbf{C}}) = 1 \\ \text{tr}(\mathbf{c}_z \mathbf{c}_z^\dagger \mathbf{R}_t) &= \text{tr}(\bar{\mathbf{C}}\mathbf{R}_t) = \delta_t \\ \text{tr}(\mathbf{c}_z \mathbf{c}_z^\dagger \mathbf{R}_s) &= \text{tr}(\bar{\mathbf{C}}\mathbf{R}_s) = \delta_s \\ \text{tr}(\mathbf{c}_z \mathbf{c}_z^\dagger \mathbf{C}_0) &= \text{tr}(\bar{\mathbf{C}}\mathbf{C}_0) = \delta_\epsilon \end{aligned} \quad (21)$$

namely feasible for EQP. Hence, given  $H$  different vectors  $\mathbf{z} \notin \text{range}(\bar{\mathbf{C}})$ , which can be randomly generated so that  $\text{rank}(\bar{\mathbf{C}} + \mathbf{z}\mathbf{z}^\dagger) = 3$ , we can get  $H$  feasible solutions of EQP and, then, we can select the one which has the largest objective function value. Besides the randomized way to generate feasible solutions, which is suboptimal, we can also consider a deterministic approach. In particular, the following method provides a feasible solution with a loss of optimality by  $\bar{y}_4(\text{tr}(\mathbf{C}_0\mathbf{c}\mathbf{c}^\dagger) - \delta_\epsilon)$ :

- 1) perform the rank-one decomposition  $[\mathbf{c}_1, \mathbf{c}_2] = \mathcal{D}_2(\bar{\mathbf{C}}, \delta_t \mathbf{I} - \mathbf{R}_t, \delta_s \mathbf{I} - \mathbf{R}_s)$ ;
- 2) choose a suboptimal solution  $\mathbf{c}$  from  $\mathbf{c}_1/\|\mathbf{c}_1\|$  or  $\mathbf{c}_2/\|\mathbf{c}_2\|$ , say  $\mathbf{c} = \mathbf{c}_1/\|\mathbf{c}_1\|$ , such that  $\text{tr}(\mathbf{C}_0\mathbf{c}\mathbf{c}^\dagger) \geq \delta_\epsilon$ .

As our simulation shows, the subcase 3.2 happens in less than 0.1% of the experiments (see Fig. 12, and we report the details of the simulation in Section IV-C).

Summarizing, the STAP code, which is optimum for problem QP (except for case 3.2), can be constructed according to Algorithm 1, pictorially illustrated in Fig. 1.

---

#### Algorithm 1: STAP Coding Algorithm

---

**Input:**  $N, M, f_s, f_t, \mathbf{M}, \mathbf{C}_0, \delta_s, \delta_t, \delta_\epsilon$ ;

**Output:**  $\mathbf{c}_{\text{STAP}}$ ;

- 1: solve the SDP problem REQP finding an optimal solution  $\bar{\mathbf{C}}$ ;
  - 2: evaluate  $R = \text{rank}(\bar{\mathbf{C}})$ ;
  - 3: **if**  $R = 1$  **then**
  - 4: evaluate  $\bar{\mathbf{c}}$  such that  $\bar{\mathbf{C}} = \bar{\mathbf{c}}\bar{\mathbf{c}}^\dagger$ ;
  - 5: **else if**  $R \geq 3$  **then**
  - 6: evaluate  $\bar{\mathbf{c}} = \mathcal{D}_4(\bar{\mathbf{C}}, \mathbf{I}, \mathbf{R}_s, \mathbf{R}_t, \mathbf{C}_0)$ ;
  - 7: **else if**  $R = 2$  **then**
  - 8:  $\bar{\mathbf{c}} = \text{Algorithm 2}(\bar{\mathbf{C}}, \mathbf{R}_s, \mathbf{R}_t, \mathbf{C}_0, \delta_s, \delta_t, \delta_\epsilon)$ ;
  - 9: **end**
  - 10:  $\mathbf{c}_{\text{STAP}} = \bar{\mathbf{c}}e^{j\phi}$ , with  $\phi = \arg(\bar{\mathbf{c}}^\dagger \mathbf{C}_0)$ .
- 

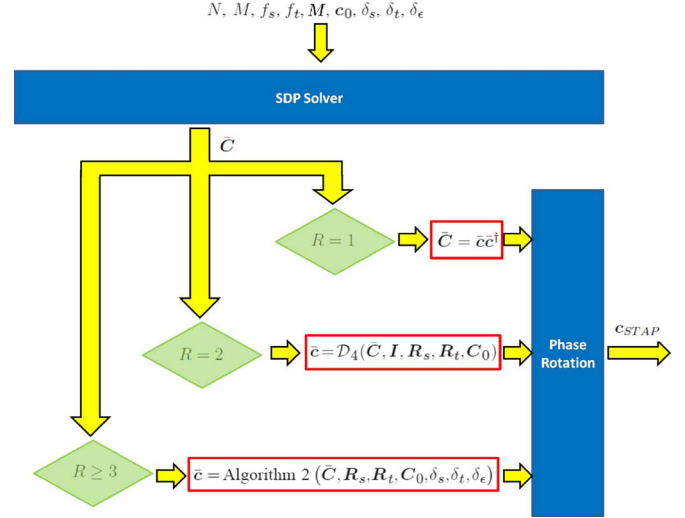


Fig. 1. Algorithm 1 for STAP coding.

---

#### Algorithm 2: EQP Feasible Solution for $R = 2$

---

**Input:**  $\bar{\mathbf{C}}, \mathbf{R}_s, \mathbf{R}_t, \mathbf{C}_0, \delta_s, \delta_t, \delta_\epsilon$

**Output:**  $\bar{\mathbf{c}}$

- 1: evaluate  $\delta_2 = \text{tr}(\bar{\mathbf{C}}\mathbf{R}_t)$ ,  $\delta_3 = \text{tr}(\bar{\mathbf{C}}\mathbf{R}_s)$  and  $\delta_4 = \text{tr}(\bar{\mathbf{C}}\mathbf{C}_0)$ ;
  - 2: **if**  $\delta_2 > \delta_t$  **then**
  - 3: evaluate  $[\mathbf{c}_1, \mathbf{c}_2] = \mathcal{D}_2(\bar{\mathbf{C}}, \delta_3 \mathbf{I} - \mathbf{R}_s, \delta_4 \mathbf{I} - \mathbf{C}_0)$ ;
  - 4: **if**  $\mathbf{c}_1^\dagger \mathbf{R}_t \mathbf{c}_1 / \|\mathbf{c}_1\|^2 > \delta_t$  **then**
  - 5: evaluate  $\bar{\mathbf{c}} = \mathbf{c}_1 / \|\mathbf{c}_1\|$ ;
  - 6: **else**
  - 7: evaluate  $\bar{\mathbf{c}} = \mathbf{c}_2 / \|\mathbf{c}_2\|$ ;
  - 8: **end**
  - 9: **else if**  $\delta_3 > \delta_s$  **then**
  - 10: evaluate  $[\mathbf{c}_1, \mathbf{c}_2] = \mathcal{D}_2(\bar{\mathbf{C}}, \delta_2 \mathbf{I} - \mathbf{R}_t, \delta_4 \mathbf{I} - \mathbf{C}_0)$ ;
  - 11: **if**  $\mathbf{c}_1^\dagger \mathbf{R}_s \mathbf{c}_1 / \|\mathbf{c}_1\|^2 > \delta_s$  **then**
  - 12: evaluate  $\bar{\mathbf{c}} = \mathbf{c}_1 / \|\mathbf{c}_1\|$ ;
  - 13: **else**
  - 14: evaluate  $\bar{\mathbf{c}} = \mathbf{c}_2 / \|\mathbf{c}_2\|$ ;
  - 15: **end**
  - 16: **else if**  $\delta_4 > \delta_\epsilon$  **then**
  - 17: evaluate  $[\mathbf{c}_1, \mathbf{c}_2] = \mathcal{D}_2(\bar{\mathbf{C}}, \delta_2 \mathbf{I} - \mathbf{R}_t, \delta_3 \mathbf{I} - \mathbf{R}_s)$ ;
  - 18: **if**  $\mathbf{c}_1^\dagger \mathbf{C}_0 \mathbf{c}_1 / \|\mathbf{c}_1\|^2 > \delta_\epsilon$  **then**
  - 19: evaluate  $\bar{\mathbf{c}} = \mathbf{c}_1 / \|\mathbf{c}_1\|$ ;
  - 20: **else**
  - 21: evaluate  $\bar{\mathbf{c}} = \mathbf{c}_2 / \|\mathbf{c}_2\|$ ;
  - 22: **end**
  - 23: **else if**  $\delta_2 = \delta_t, \delta_3 = \delta_s$  and  $\delta_4 = \delta_\epsilon$  **then**
  - 24: determine, using Proposition II,  $H$  feasible solutions  $\mathbf{c}_i$ ,  $i = 1, \dots, H$ ;
  - 25: select  $\bar{\mathbf{c}}$  from  $\{\mathbf{c}_1, \dots, \mathbf{c}_H\}$  such that  $\bar{\mathbf{c}}^\dagger \mathbf{R} \bar{\mathbf{c}} \geq \mathbf{c}_i^\dagger \mathbf{R} \mathbf{c}_i$  for all  $i = 1, \dots, H$ .
  - 26: **end**
- 

The computational complexity, connected with the implementation of the algorithm, is polynomial, since  $O(N^{3.5} \log(1/\zeta))$  is the amount of operations involved in

solving the SDP problem, and  $O(N^3)$  is the complexity required by the decompositions  $\mathcal{D}_2(\cdot, \cdot, \cdot)$  and  $\mathcal{D}_4(\cdot, \cdot, \cdot, \cdot, \cdot)$ .

#### IV. PERFORMANCE ANALYSIS

The present section is aimed at analyzing the performance of the proposed encoding scheme. The analysis is conducted in terms of detection probability ( $P_d$ ), regions of achievable Doppler estimation accuracies ( $\mathcal{A}_t$  and  $\mathcal{A}_s$ ), and ambiguity function of the pulse train modulated through the proposed code  $\bar{\mathbf{c}}$ . To proceed further we recall that, for a specified value of the false alarm probability ( $P_{fa}$ ), and for nonfluctuating target [33],  $P_d$  can be evaluated as

$$P_d = Q\left(\sqrt{2|\alpha|^2 \bar{\mathbf{c}}^\dagger \mathbf{R} \bar{\mathbf{c}}}, \sqrt{-2 \ln P_{fa}}\right) \quad (22)$$

where  $Q(\cdot, \cdot)$  is the Marcum  $Q$  function of order 1. As benchmark code for the detection probability, we consider the unconstrained unitary code

$$\mathbf{c}_{\text{benchmark}} = \arg \max_{\mathbf{c}} \{ \mathbf{c}^\dagger \mathbf{R} \mathbf{c} \mid \|\mathbf{c}\|^2 = 1 \} \quad (23)$$

which does not necessarily satisfy the similarity constraints or spatial/temporal Doppler accuracy constraints. Since that  $\mathbf{c}_{\text{benchmark}}^\dagger \mathbf{R} \mathbf{c}_{\text{benchmark}} = \lambda_{\max}(\mathbf{R})$ , where  $\lambda_{\max}(\cdot)$  is the maximum eigenvalue of the matrix argument, the benchmark  $P_d$  can be expressed as

$$P_d^{\text{benchmark}} = Q\left(\sqrt{2|\alpha|^2 \lambda_{\max}(\mathbf{R})}, \sqrt{-2 \ln P_{fa}}\right). \quad (24)$$

Analogously, we consider a benchmark CRB for both spatial and temporal Doppler frequencies, i.e.,

$$\text{CRB}_l^{\text{benchmark}} = \frac{\Psi}{\lambda_{\max}(\mathbf{R}_l)}, \quad l \in \{s, t\}. \quad (25)$$

Notice that, in general, the three values  $P_d^{\text{benchmark}}$ ,  $\text{CRB}_s^{\text{benchmark}}$ , and  $\text{CRB}_t^{\text{benchmark}}$  are not obtained in correspondence of the same unitary norm code.

Besides, the ambiguity function of the coded pulse train can be evaluated as

$$\begin{aligned} \chi(\tau, \nu) &= \int_{-\infty}^{\infty} u(\beta) u^*(\beta - \tau) e^{j2\pi\nu\beta} d\beta \\ &= \sum_{m=0}^{N-1} \sum_{n=0}^{N-1} \bar{\mathbf{c}}(m) \bar{\mathbf{c}}^*(n) \chi_p(\tau - (m-n)T_r, \nu) \end{aligned}$$

where  $[\bar{\mathbf{c}}(0), \dots, \bar{\mathbf{c}}(N-1)]^T = \bar{\mathbf{c}}$ , and  $\chi_p(\cdot, \cdot)$  is the ambiguity function of an unmodulated pulse [12].

In our scenario, we consider a STAP system with  $M = 11$  channels and  $N = 32$  pulses. Moreover, we fix  $P_{fa}$  to  $10^{-6}$ . As to the temporal steering vector  $\mathbf{p}_t$ , we set the normalized temporal Doppler frequency  $f_t = 0.25$ , while we use the normalized spatial Doppler frequency  $f_s = 0.15$  for the spatial steering vector  $\mathbf{p}_s$ . As similarity code  $\mathbf{c}_0$ , we resort to a generalized Barker sequence [12, pp. 109-113]: such codes are polyphase

sequences whose autocorrelation function has minimal peak-to-sidelobe ratio excluding the outermost sidelobe. Examples of these sequences have been found for all  $N \leq 45$  [34], [35], using numerical optimization techniques. In our simulations, we choose a unitary norm version of the generalized Barker code  $\mathbf{c}_0$  of length 32 reported in [12, p. 111].

In order to compare the performance of our algorithm with that of the similarity code, we have also evaluated  $P_d$  and CRBs obtained using  $\mathbf{c}_0$ , i.e.,

$$P_d^0 = Q\left(\sqrt{2|\alpha|^2 \mathbf{c}_0^\dagger \mathbf{R} \mathbf{c}_0}, \sqrt{-2 \ln P_{fa}}\right) \quad (26)$$

and

$$\text{CRB}_l^0 = \frac{\Psi}{\mathbf{c}_0^\dagger \mathbf{R}_l \mathbf{c}_0}, \quad l \in \{s, t\}. \quad (27)$$

Concerning the inverse disturbance covariance matrix  $\mathbf{M}$ , we consider the two following scenarios:

- 1) simulated covariance, according to the disturbance model described in [23];
- 2) covariance, from the KASSPER database [28].

Regarding the parameters  $\delta_t$  and  $\delta_s$ , in general, what can be assigned is the interval of  $\delta_s$  and  $\delta_t$  values which can be exploited. Evidently, they depend on  $\mathbf{M}$ ,  $f_s$ , and  $f_t$  and must be smaller than the maximum eigenvalue of  $\mathbf{R}_s$  and  $\mathbf{R}_t$  respectively. From a practical point of view, the selection of the quoted parameters depend on the desired accuracy region (provided it is compatible with strict feasibility). In the numerical examples, we have considered a wide variation range for the parameters so as to better highlight the performance tradeoff due to different parameters combinations.

Finally, in the numerical simulations, we have exploited the MATLAB toolbox SeDuMi [36] for solving the SDP relaxation, and the MATLAB toolbox of [37] for plotting the ambiguity functions of the coded pulse trains.

#### A. Simulated Covariance

The disturbance covariance matrix  $\mathbf{M}^{-1}$  has been simulated according to the model in [23, ch. 2], as the sum of a clutter term plus a thermal noise contribution, i.e.,  $\mathbf{M}^{-1} = \mathbf{R}_{\text{clutter}} + \sigma^2 \mathbf{I}$ , where  $\mathbf{R}_{\text{clutter}}$  is the clutter covariance and  $\sigma^2$  is the thermal noise level. More precisely,  $\mathbf{R}_{\text{clutter}}$  can be obtained using the general clutter model described in [23, par. 2.6.1]. It accounts for the effects of velocity misalignment (due to aircraft crab) and intrinsic clutter motion [23]. A synthetic description of the principal radar system parameters, used in the simulations, is reported in Table I (for a more exhaustive list, please refer to [23]).

In Fig. 2(a), we plot  $P_d$  of the optimum code (according to the proposed criterion) versus  $|\alpha|^2$  for nonfluctuating target,  $\delta_s = 3.8$ ,  $\delta_e = 0.001$ , and for several values of  $\delta_t$ . In the same figure, we also represent both the  $P_d^0$  and the  $P_d^{\text{benchmark}}$ . The curves show that, increasing  $\delta_t$ , we get lower and lower values of  $P_d$  for a given  $|\alpha|^2$  value. This was expected since the higher  $\delta_t$  the smaller the feasibility region of the optimization problem

TABLE I  
RADAR SYSTEM PARAMETERS

Peak power	200 kW	Transmit Gain	21 dB
Pulse width	0.2 ms	Receiver Gain	10 dB
System Losses	4 dB	Instantaneous Bandwidth	4 MHz
Operating frequency	300 MHz	Noise Figure	3 dB
PRF	300 Hz	Clutter-to-Noise Ratio	30 dB
Duty Factor	6%	Number of clutter foldovers	$\beta = 1$
Platform Velocity	50 m/s	Platform Altitude	9000 m

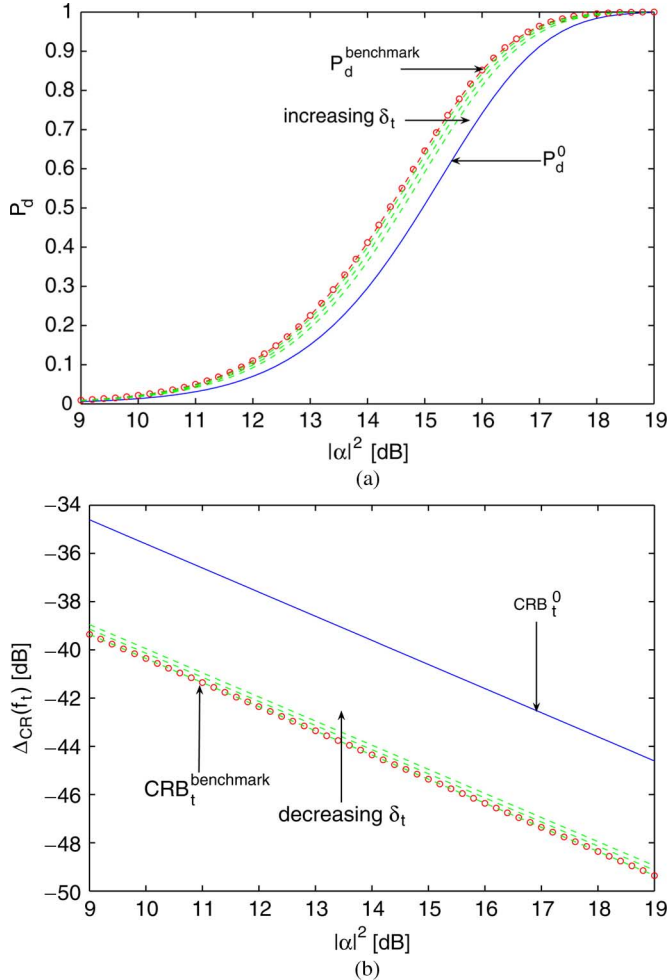


Fig. 2. (a)  $P_d$  versus  $|\alpha|^2$  for nonfluctuating target, simulated data,  $P_{fa} = 10^{-6}$ ,  $N = 32$ ,  $M = 11$ ,  $f_t = 0.25$ ,  $f_s = 0.15$ ,  $\delta_s = 3.8$ ,  $\delta_e = 0.001$ , and several values of  $\delta_t \in \{494.4, 516.0, 543.0\}$ . Generalized Barker code (solid curve).  $P_d$  of the proposed code for a given  $\delta_t$  (dashed curves). Benchmark  $P_d$  (o-marked dashed curve). (b)  $\Delta_{CR}(f_t)$  versus  $|\alpha|^2$  for nonfluctuating target, simulated data,  $f_t = 0.25$ ,  $f_s = 0.15$ ,  $N = 32$ ,  $M = 11$ ,  $\delta_s = 3.8$ ,  $\delta_e = 0.001$ , and several values of  $\delta_t \in \{494.4, 516.0, 543.0\}$ . Generalized Barker code (solid curve).  $\Delta_{CR}(f_t)$  of the proposed code for a given  $\delta_t$  (dashed curves). Benchmark  $\Delta_{CR}(f_t)$  (o-marked dashed curve).

to be solved for finding the code. Nevertheless, the proposed encoding algorithm usually ensures a better detection performance than the original generalized Barker code.

In Fig. 2(b),  $\Delta_{CR}(f_t)$  is plotted versus  $|\alpha|^2$  for the same values of  $\delta_t$  as in Fig. 2(a). The benchmark  $CRB_t$  and  $CRB_t^0$  are plotted too. The curves highlight that, increasing  $\delta_t$ , better and

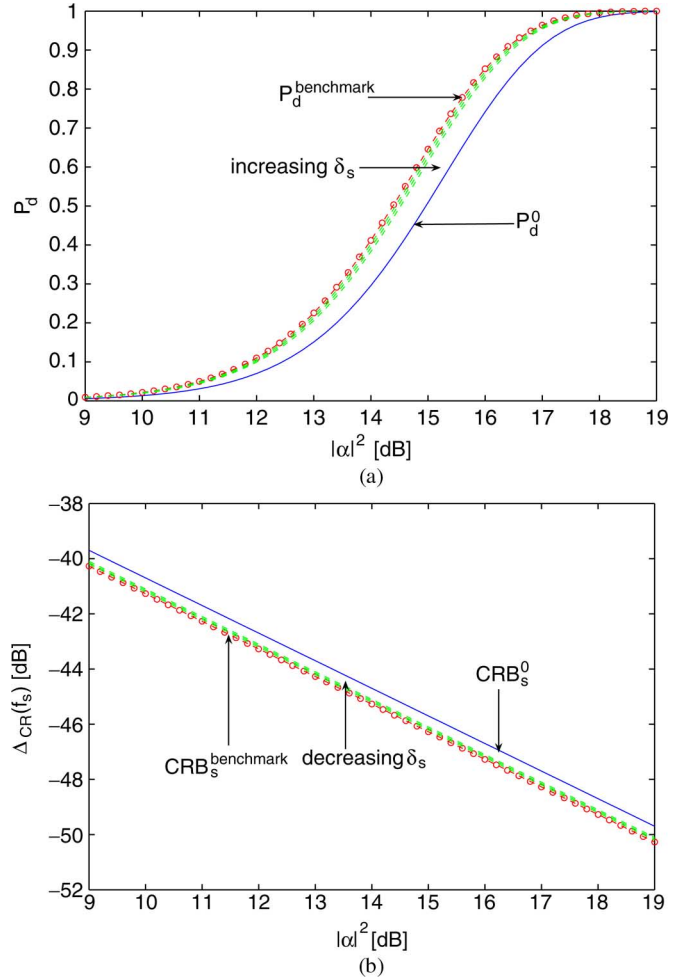


Fig. 3. (a)  $P_d$  versus  $|\alpha|^2$  for nonfluctuating target, simulated data,  $P_{fa} = 10^{-6}$ ,  $N = 32$ ,  $M = 11$ ,  $f_t = 0.25$ ,  $f_s = 0.15$ ,  $\delta_t = 0.5$ ,  $\delta_e = 0.001$ , and several values of  $\delta_s \in \{656.7, 658.9, 669.9\}$ . Generalized Barker code (solid curve).  $P_d$  of the proposed code for a given  $\delta_s$  (dashed curves). Benchmark  $P_d$  (o-marked dashed curve). (b)  $\Delta_{CR}(f_s)$  versus  $|\alpha|^2$  for nonfluctuating target, simulated data,  $N = 32$ ,  $M = 11$ ,  $f_t = 0.25$ ,  $f_s = 0.15$ ,  $\delta_t = 0.5$ ,  $\delta_e = 0.001$ , and several values of  $\delta_s \in \{656.7, 658.9, 669.9\}$ . Generalized Barker code (solid curve).  $\Delta_{CR}(f_s)$  of the proposed code for a given  $\delta_s$  (dashed curves). Benchmark  $\Delta_{CR}(f_s)$  (o-marked dashed curve).

better  $\Delta_{CR}(f_t)$  values can be achieved. This is in accordance with the considered criterion, because the higher  $\delta_t$  the larger the size of the region  $\mathcal{A}_t$ .

In Fig. 3(a), we plot  $P_d$  versus  $|\alpha|^2$  for nonfluctuating target,  $\delta_t = 0.5$ ,  $\delta_e = 0.001$ , and for several values of  $\delta_s$ . Also in this case, we can notice a gain of the proposed encoding scheme over the classic generalized Barker code. However, the gain slightly reduces as the parameter  $\delta_s$  increases, since the feasibility region becomes smaller and smaller.

In Fig. 3(b), we plot  $CRB_s^{\text{benchmark}}$ ,  $CRB_s^0$  and  $\Delta_{CR}(f_s)$  versus  $|\alpha|^2$  for the same values of the parameters considered in the previous figure. We observe that increasing  $\delta_s$ , we slightly enlarge the region of achievable spatial Doppler accuracy. Moreover, the proposed encoding technique assures a larger  $\mathcal{A}_s$  than the generalized Barker code.

Summarizing, the joint analysis of Figs. 2 and 3 shows that a tradeoff can be realized between the detection performance and the estimation accuracy of both the temporal and the spatial

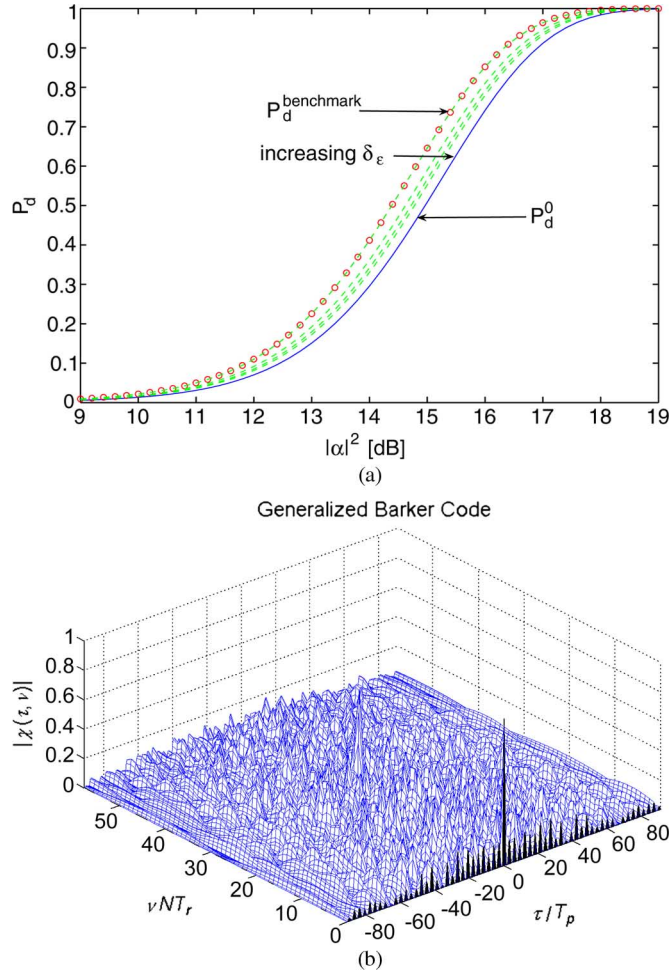


Fig. 4. (a)  $P_d$  versus  $|\alpha|^2$  for nonfluctuating target, simulated data,  $P_{fa} = 10^{-6}$ ,  $N = 32$ ,  $M = 11$ ,  $f_t = 0.25$ ,  $f_s = 0.15$ ,  $\delta_t = 0.5$ ,  $\delta_s = 3.8$ , and several values of  $\delta_\epsilon \in \{0, 0.9811, 0.9918, 0.9957\}$ . Generalized Barker code (solid curve).  $P_d$  of the proposed code for a given  $\delta_\epsilon$  (dashed curves). Benchmark  $P_d$  (o-marked dashed curve). (b) Ambiguity function modulus of the generalized Barker code  $\mathbf{c}_0$  with  $T_r = 3T_p$ .

Doppler frequencies. Additionally, there exist codes capable of outperforming the generalized Barker code both in terms of  $P_d$  and sizes of  $\mathcal{A}_t$  and  $\mathcal{A}_s$ .

The effects of the similarity constraint are analyzed in Fig. 4(a). Therein, we set  $\delta_t = 0.5$ ,  $\delta_s = 3.8$ , and consider several values of  $\delta_\epsilon$ . The plots show that increasing  $\delta_\epsilon$  worse and worse  $P_d$  values are obtained; this behavior can be explained observing that the smaller  $\delta_\epsilon$  the larger the size of the similarity region. However, this detection loss is compensated for an improvement of the coded pulse train ambiguity function, as we can see in Fig. 5(a)–(d), where the modulus of that function is plotted assuming rectangular pulses, and  $T_r = 3T_p$ . For comparison purposes, the ambiguity function modulus of  $\mathbf{c}_0$  is plotted in Fig. 4(b). The plots highlight that the closer  $\delta_\epsilon$  to 1 the higher the degree of similarity between the ambiguity functions of the devised and pre-fixed codes. This is due to the fact that increasing  $\delta_\epsilon$  is tantamount to reducing the size of the similarity region. In other words, we force the devised code to be similar and similar to the pre-fixed one and, as a consequence, we get closer and closer ambiguity functions.

In the previous figures, we have fixed two parameters, and have changed the other in order to analyze the impact on the performance of a particular constraint. In Fig. 6, we analyze the joint effect of the three parameters, so as to show that there are situations where the proposed encoding method can outperform the generalized Barker coding in terms of  $P_d$ ,  $\Delta_{CR}(f_t)$ , and  $\Delta_{CR}(f_s)$ . In particular, in Fig. 6(a) we plot  $P_d$ , in Fig. 6(b)  $\Delta_{CR}(f_t)$ , and in Fig. 6(c)  $\Delta_{CR}(f_s)$  versus  $|\alpha|^2$ , assuming  $(\delta_t, \delta_s, \delta_\epsilon) = (325.7, 403.2, 0.8)$ . Evidently, for the considered values of the parameters, the proposed code, whose ambiguity function is plotted in Fig. 7, outperforms the generalized Barker in terms of  $P_d$ ,  $CRB_t$ , and  $CRB_s$ .

As to the robustness of the proposed method, we study the behavior of the algorithm when a mismatch on the temporal or spatial Doppler is present. In particular, we design two codes, one assuming  $f_t = 0.25$  and  $f_s = 0.15$ , and another where  $f_t$  and  $f_s$  are modeled as random parameter uniformly distributed in the interval  $[-1/3; 1/3]$ , i.e.,  $f_t \sim \mathcal{U}[-1/3; 1/3]$  and  $f_s \sim \mathcal{U}[-1/3; 1/3]$ . We analyze the performance when  $f_t$  (left column) or  $f_s$  (right column) ranges in the interval  $[-1/2; 1/2]$ . In Fig. 8(a) and (b), we plot the  $P_d$  versus  $f_t(f_s)$  for  $|\alpha|^2 = 14$  dB and  $(\delta_t, \delta_s, \delta_\epsilon) = (53.4, 15.6, 0.5)$ . We can notice that the proposed method outperforms the generalized Barker code almost everywhere for the case of a spatial or temporal Doppler mismatch. In other words, simulations indicate that the novel encoding method shares an intrinsic robust behavior.

### B. Covariance From the KASSPER Database

In this subsection, we use the ground clutter covariance matrix from the range cell number 10 of the KASSPER [28] database. This dataset contains many real-world effects including heterogeneous terrain, subspace leakage, array errors, and many ground targets. It refers to a California site characterized by large mountains and moderate density of roads. The chosen matrix is loaded with the thermal noise covariance matrix and then the sum is inverted to get  $\mathbf{M}^{-1}$ . As in the previous scenario, we set the clutter-to-noise ratio to 30 dB.

In Fig. 9(a) and (b), we study the effect of the parameter  $\delta_t$  on  $P_d$  and  $\Delta_{CR}(f_t)$ . In particular, in Fig. 9(a), we plot  $P_d$  of the optimum code versus  $|\alpha|^2$  for nonfluctuating target,  $\delta_s = 30.6$ ,  $\delta_\epsilon = 0.001$ , and for several values of  $\delta_t$ . In the same figure, we also represent both  $P_d^0$  and  $P_d^{\text{benchmark}}$ . We can observe a similar behavior as in the simulated case of Section IV-A: increasing  $\delta_t$ , we get lower and lower values of  $P_d$  for a given  $|\alpha|^2$  value. Moreover, our proposed encoding scheme can achieve a better detection performance than the classic generalized Barker code. In Fig. 9(b),  $\Delta_{CR}(f_t)$  is plotted versus  $|\alpha|^2$  for the same values of  $\delta_t$  as in Fig. 9(a). The benchmark  $CRB_t$  and  $CRB_t^0$  are plotted too. As expected, the curves show that increasing  $\delta_t$  better and better  $\Delta_{CR}(f_t)$  values can be obtained.

In Fig. 10(a), we plot  $P_d$  versus  $|\alpha|^2$  for nonfluctuating target,  $\delta_t = 1.1$ ,  $\delta_\epsilon = 0.001$ , and for several values of  $\delta_s$ . It is evident that an increase of the parameter  $\delta_s$  leads to a slight deterioration of detection performances. This can be explained observing that the feasibility region becomes smaller and smaller as  $\delta_s$  increases.

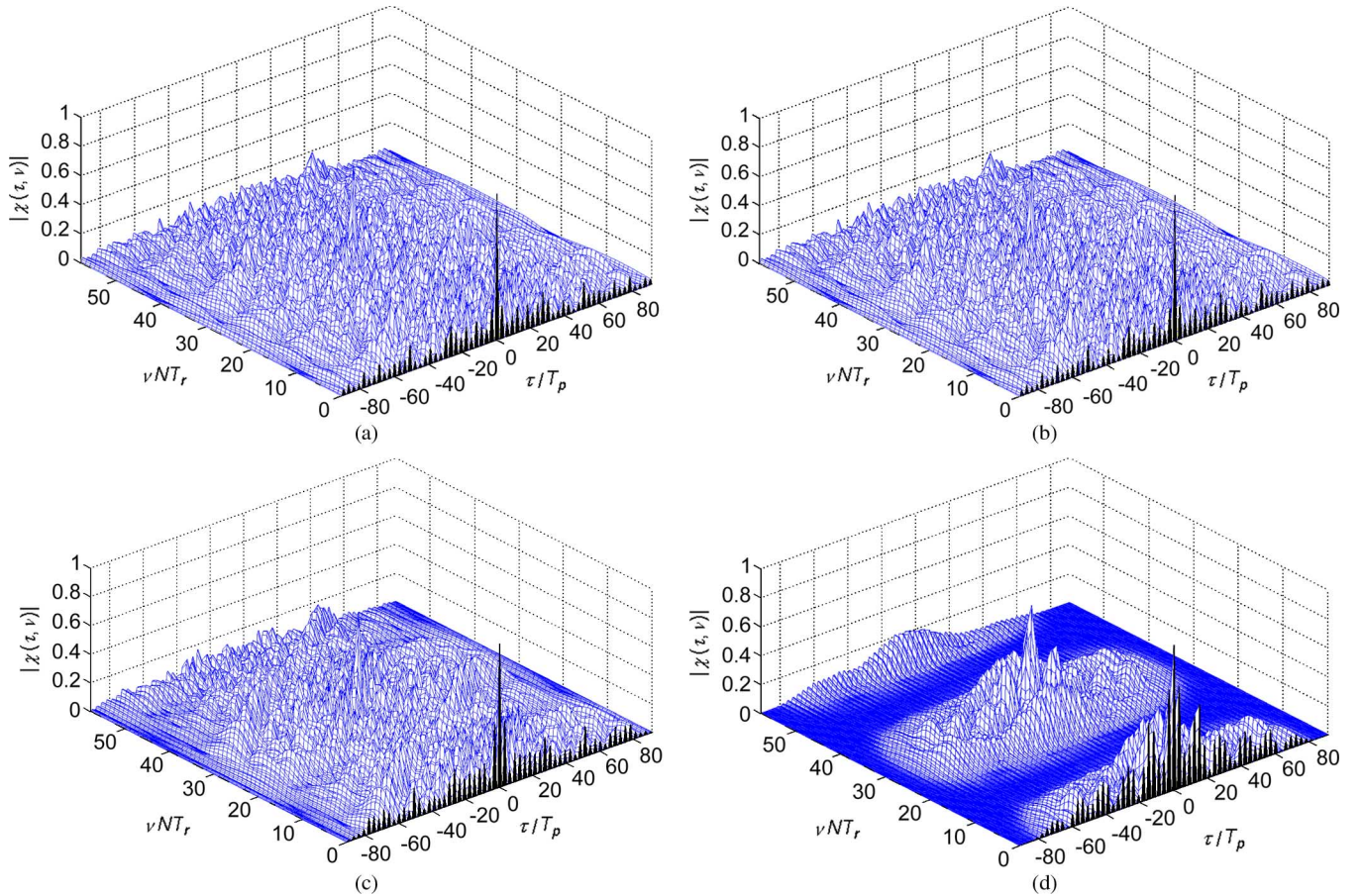


Fig. 5. (a) Ambiguity function modulus of code which maximizes the SINR for  $N = 32$ ,  $T_r = 3T_p$ ,  $\delta_t = 0.5$ ,  $\delta_s = 3.8$ ,  $c_0$  generalized Barker code, and  $\delta_\epsilon = 0.9957$ . (b) Ambiguity function modulus of code which maximizes the SINR for  $N = 32$ ,  $T_r = 3T_p$ ,  $\delta_t = 0.5$ ,  $\delta_s = 3.8$ ,  $c_0$  generalized Barker code, and  $\delta_\epsilon = 0.9918$ . (c) Ambiguity function modulus of code which maximizes the SINR for  $N = 32$ ,  $T_r = 3T_p$ ,  $\delta_t = 0.5$ ,  $\delta_s = 3.8$ ,  $c_0$  generalized Barker code, and  $\delta_\epsilon = 0.9811$ . (d) Ambiguity function modulus of code which maximizes the SINR for  $N = 32$ ,  $T_r = 3T_p$ ,  $\delta_t = 0.5$ ,  $\delta_s = 3.8$ ,  $c_0$  generalized Barker code, and  $\delta_\epsilon = 0$ .

In Fig. 10(b), we plot  $\text{CRB}_s^{\text{benchmark}}$ ,  $\text{CRB}_s^0$ , and  $\Delta_{\text{CR}}(f_s)$  versus  $|\alpha|^2$  for the same values of the parameters considered in the previous figure. The curves highlight that increasing  $\delta_s$  lower and lower  $\Delta_{\text{CR}}(f_s)$  values can be achieved.

Finally, in Fig. 11, we plot  $P_d$  versus  $|\alpha|^2$  for nonfluctuating target,  $\delta_t = 1.1$ ,  $\delta_s = 30.6$ , and for several values of  $\delta_\epsilon$ . We can notice that the closer  $\delta_\epsilon$  to 1, the closer  $P_d$  to  $P_d^0$ , namely the performances of the proposed code and the generalized Barker code end up coincident.

In conclusion,  $P_d$ ,  $\Delta_{\text{CR}}(f_t)$ , and  $\Delta_{\text{CR}}(f_s)$  exhibit a similar behavior both with simulated and KASSPER covariance data. Moreover, the proposed analysis shows that it is possible to realize a tradeoff among the three parameters  $\delta_t$ ,  $\delta_s$ , and  $\delta_\epsilon$  to increase the detection performance, or to improve the Doppler estimation accuracy, or to shape the ambiguity function.

### C. Occurrence of Subcase 3.2

In this subsection, we analyze the typical rank of an optimal solution  $\bar{\mathbf{C}}$  of the SDP problem REQ. First of all, we have to deal with the finite precision of MATLAB implementation of the encoding algorithm. To this end, we introduce the  $\text{Rank}_\gamma(\mathbf{A})$  function, namely the number of eigenvalues of the matrix  $\mathbf{A}$  greater than the positive threshold  $\gamma$ . For a positive semidefinite

matrix  $\mathbf{A}$ ,  $\text{Rank}_\gamma(\mathbf{A})$  represents a good numerical estimation of the rank of  $\mathbf{A}$ , as  $\gamma \rightarrow 0$ . Moreover, we have to distinguish a *tight* constraint from a *strict* constraint. In this case, we consider the constraint as *practically tight* if the difference of the two sides of the inequality is less than  $\gamma$ . Performing 10 000 instances of the problem REQ (with clutter covariance matrix from the range cell number 10 of the KASSPER datacube,  $M = 11$ ,  $N = 32$ ,  $f_t = 0.25$ ,  $f_s = 0.15$ ,  $c_0$  generalized Barker sequence,  $\delta_t$ ,  $\delta_s$ , and  $\delta_\epsilon$  randomly chosen),<sup>5</sup> in less than 1% of the cases, we get an optimal solution  $\bar{\mathbf{C}}$  with  $\text{Rank}_\gamma(\bar{\mathbf{C}}) = 2$ . For those particular situations, we have also controlled the constraints, and in less than 10% of the cases, we have all the three constraints *practically tight* (namely, case 3.2 described in Section III). Summarizing, in less than 0.1% of the instances, we have a suboptimal solution of the original QP problem. This trend holds for all the considered values of the parameter  $\gamma$ .<sup>6</sup> Furthermore, most of the instances presents a  $\text{Rank}_\gamma(\bar{\mathbf{C}}) = 1$ , even if the number decreases as the precision  $\gamma$  tends to 0 (and consequently the occurrence of the event  $\text{Rank}_\gamma(\bar{\mathbf{C}}) \geq 3$  increases). Thus, we

<sup>5</sup> $\delta_t$  is a uniformly distributed random variable in the interval  $[\lambda_{\min}(\mathbf{R}_t); \lambda_{\max}(\mathbf{R}_t)]$ ,  $\delta_s$  in  $[\lambda_{\min}(\mathbf{R}_s); \lambda_{\max}(\mathbf{R}_s)]$ , and  $\delta_\epsilon$  in  $[0; 1]$ , with  $\lambda_{\min}(\cdot)$  representing the minimum eigenvalue of the argument.

<sup>6</sup>Notice that additional results obtained changing  $M$  and  $c_0$  randomly in the 10 000 experiments also agree with the aforementioned behavior.

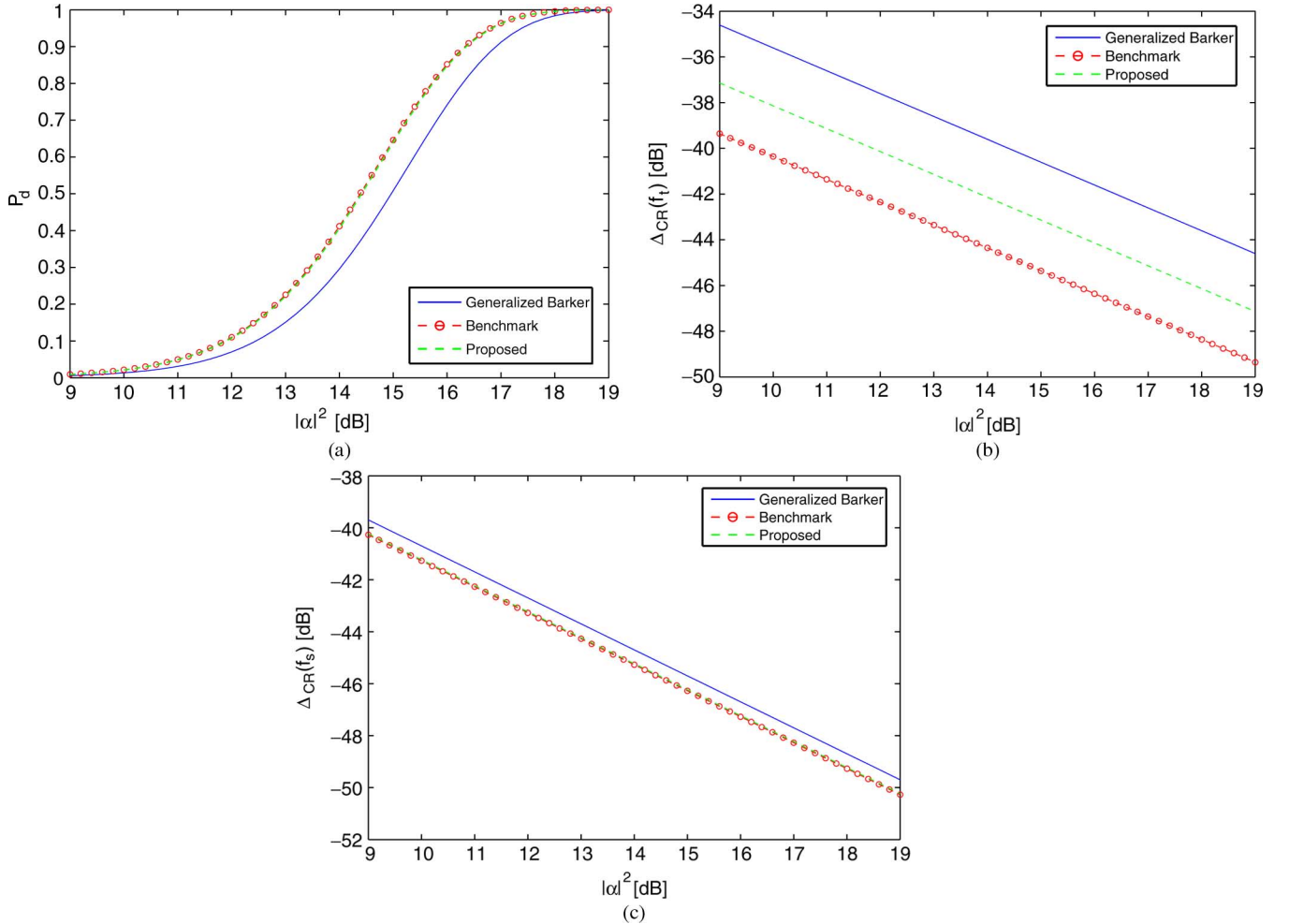


Fig. 6. (a)  $P_d$  versus  $|\alpha|^2$  for nonfluctuating target, simulated data,  $P_{fa} = 10^{-6}$ ,  $N = 32$ ,  $M = 11$ ,  $f_t = 0.25$ ,  $f_s = 0.15$ , and  $(\delta_t, \delta_s, \delta_\epsilon) = (325.7, 403.2, 0.8)$ .  $P_d$  of the proposed code (dashed curves). Benchmark  $P_d$  (o-marked dashed curve). (b)  $\Delta_{CR}(f_t)$  versus  $|\alpha|^2$  for nonfluctuating target, simulated data,  $f_t = 0.25$ ,  $f_s = 0.15$ ,  $N = 32$ ,  $M = 11$ , and  $(\delta_t, \delta_s, \delta_\epsilon) = (325.7, 403.2, 0.8)$ .  $\Delta_{CR}(f_t)$  of the proposed code (dashed curves). Benchmark  $\Delta_{CR}(f_t)$  (o-marked dashed curve). (c)  $\Delta_{CR}(f_s)$  versus  $|\alpha|^2$  for nonfluctuating target, simulated data,  $N = 32$ ,  $M = 11$ ,  $f_t = 0.25$ ,  $f_s = 0.15$ , and  $(\delta_t, \delta_s, \delta_\epsilon) = (325.7, 403.2, 0.8)$ .  $\Delta_{CR}(f_s)$  of the proposed code (dashed curves). Benchmark  $\Delta_{CR}(f_s)$  (o-marked dashed curve).

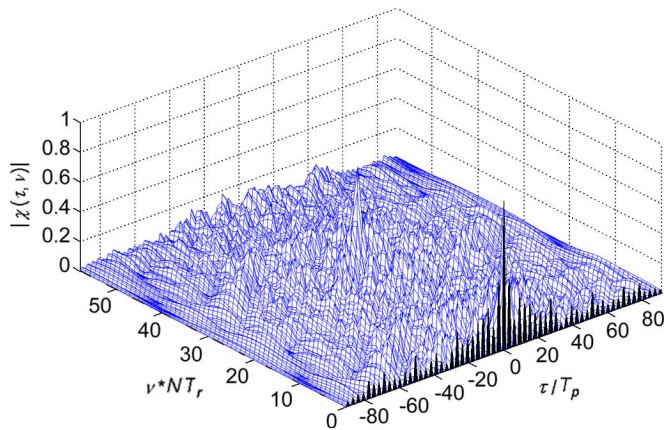


Fig. 7. Ambiguity function modulus of proposed code for  $N = 32$ ,  $T_r = 3T_p$ ,  $c_0$  generalized Barker code, and  $(\delta_t, \delta_s, \delta_\epsilon) = (325.7, 403.2, 0.8)$ .

can conclude observing that a duality gap between the original problem QP and the relaxed problem REQP (namely an optimal solution of rank 2 and all the constraints tight) is very rare, and even for high precision (i.e.,  $\gamma = 10^{-8}$ ), it happens in less than 0.1% of the cases. The analysis is summarized in Fig. 12.

## V. CONCLUSION

In this paper, we have addressed the problem of code design for radar STAP, assuming that the overall disturbance component, which contaminates the useful signal, is a colored complex circular Gaussian vector. We have considered the class of linearly coded pulse trains and have determined the radar code which maximizes the detection performance under a constraint on the region of achievable values for the temporal and spatial Doppler estimation accuracy and forcing a similarity constraint with a given radar code exhibiting some desirable properties.

The optimization problem, we have been faced with, is nonconvex and quadratic. In order to solve it, we have first performed a relaxation into a convex SDP problem. Then, applying appropriately the rank-one decomposition theorems of [26] and [27] to an optimal solution of the relaxed problem, we have determined an optimal code. Remarkably, the proposed code design procedure requires a polynomial computational complexity.

At the analysis stage, we have assessed the performance of the new algorithm both on simulated data and on the KASSPER reference STAP datacube. The analysis has been conducted in

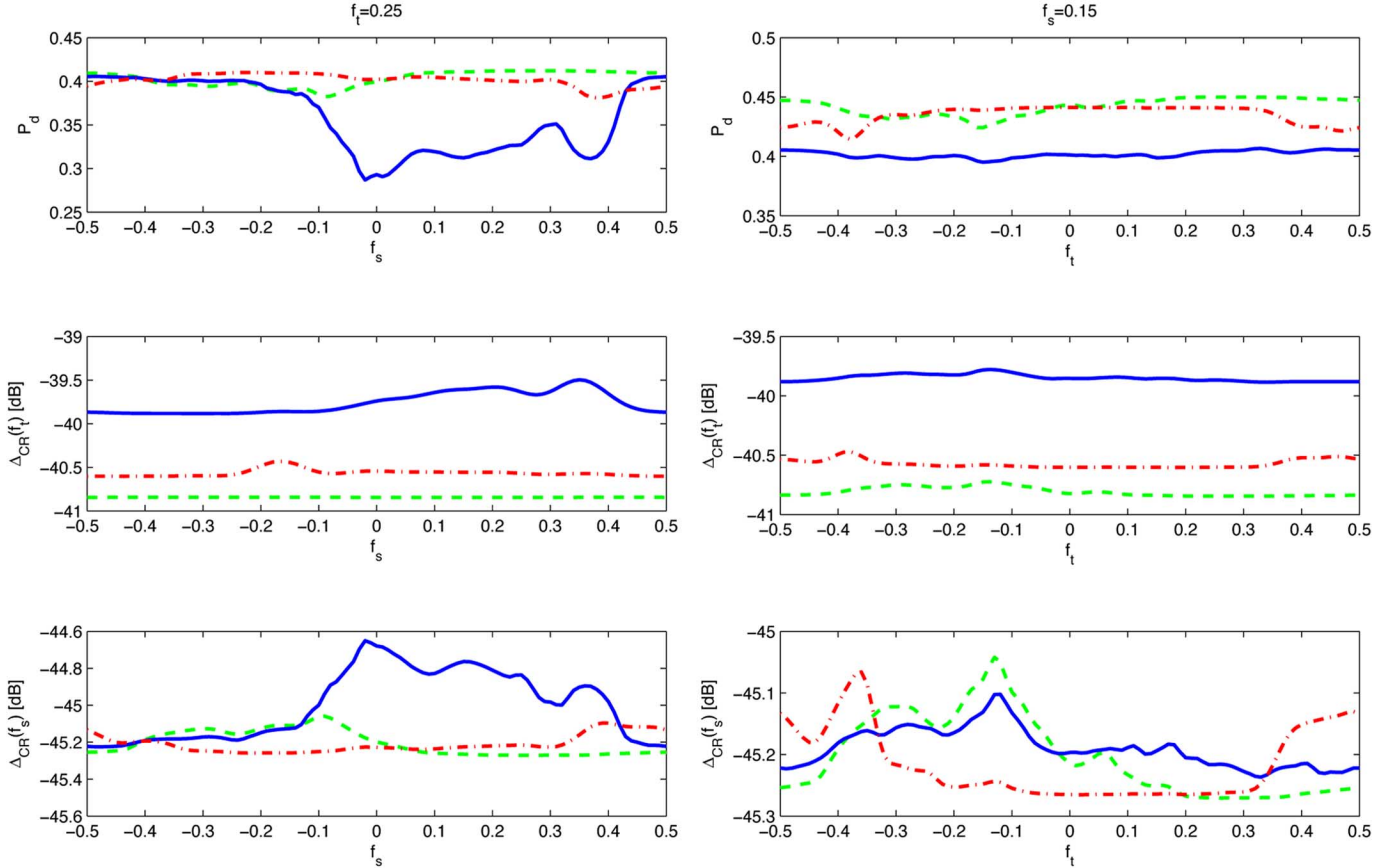


Fig. 8. Robustness analysis for  $|\alpha|^2 = 14$  dB, nonfluctuating target, simulated data,  $N = 32$ ,  $M = 11$ ,  $(\delta_t, \delta_s, \delta_\epsilon) = (53.4, 15.6, 0.5)$ ,  $f_t = 0.25$  and  $f_s \in [-1/2; 1/2]$  (left column),  $f_s = 0.15$  and  $f_t \in [-1/2; 1/2]$  (right column). Proposed code for  $f_t = 0.25$  and  $f_s = 0.15$  (dashed curves), Generalized Barker code (solid curves), Proposed code for  $f_t \sim U[-1/3; 1/3]$  and  $f_s \sim U[-1/3; 1/3]$  (dashed-dotted curves). (a)  $P_d$  versus  $f_t$ ; (b)  $P_d$  versus  $f_s$ ; (c)  $\Delta_{CR}(f_t)$  versus  $f_t$ ; (d)  $\Delta_{CR}(f_t)$  versus  $f_s$ ; (e)  $\Delta_{CR}(f_s)$  versus  $f_t$ ; (f)  $\Delta_{CR}(f_s)$  versus  $f_s$ .

terms of detection performance, regions of estimation accuracies that unbiased estimators of the temporal and the spatial Doppler frequencies can theoretically achieve, and ambiguity function. The results have highlighted the tradeoff existing among the aforementioned performance metrics. Otherwise stated, detection capabilities can be traded with desirable properties of the coded waveform and/or with enlarged regions of achievable temporal/spatial Doppler estimation accuracies.

Possible future research tracks might concern the possibility to make the algorithm adaptive with respect to the disturbance covariance matrix, namely to devise techniques which jointly estimate the code and the covariance. Moreover, it should be investigated the introduction in the code design optimization problem of constraints related to the probability of correct target classification as well as of knowledge-based constraints, ruled by the *a priori* information that the radar has about the surrounding environment. Finally, it might also be of interest to consider the case of a MIMO system [38]–[40] equipped with multiple transmitters (possibly not colocated) and/or receivers, and of an over-the-horizon (OTH) radar scenario.

## APPENDIX

### A. Proof of Lemma I

*Proof:* Since  $(\mathbf{c} \odot \mathbf{a}) \otimes \mathbf{b} = (\mathbf{I} \otimes \mathbf{b})(\mathbf{c} \odot \mathbf{a})$ ,  $[(\mathbf{c} \odot \mathbf{a}) \otimes \mathbf{b}]^\dagger \mathbf{M}[(\mathbf{c} \odot \mathbf{a}) \otimes \mathbf{b}] = (\mathbf{c} \odot \mathbf{a})^\dagger [(\mathbf{I} \otimes \mathbf{b})^\dagger \mathbf{M}(\mathbf{I} \otimes \mathbf{b})](\mathbf{c} \odot \mathbf{a})$  which

can be recast as  $\mathbf{c}^\dagger \mathbf{R} \mathbf{c}$  with  $\mathbf{R}$  given by (4). It is evident that  $\mathbf{M} \succeq \mathbf{0}$  implies  $\mathbf{R} \succeq \mathbf{0}$ . Moreover, if  $\mathbf{M} \succ \mathbf{0}$ , all the entries of  $\mathbf{a}$  are nonzero, and  $\mathbf{b} \neq \mathbf{0}$  (i.e., at least one of its component is nonzero), then, for any nonzero  $\mathbf{c} \in \mathbb{C}^N$ ,  $(\mathbf{c} \odot \mathbf{a}) \otimes \mathbf{b} \neq \mathbf{0}$  and, as a consequence,  $\mathbf{c}^\dagger \mathbf{R} \mathbf{c} = [(\mathbf{c} \odot \mathbf{a}) \otimes \mathbf{b}]^\dagger \mathbf{M}[(\mathbf{c} \odot \mathbf{a}) \otimes \mathbf{b}] > 0$ , namely  $\mathbf{R} \succ \mathbf{0}$ . Finally, if  $\mathbf{M} \succ \mathbf{0}$  and at least one entry of  $\mathbf{a}$  is equal to zero, then  $\mathbf{R}$  shares at least a column and a row with all zero entries, implying  $\mathbf{R} \succeq \mathbf{0}$ .

### B. Proof of Lemma II

*Proof:* First, we note that an optimal solution of EQP or QP must exist, since the feasible sets are compact and the objective function of EQP or QP is continuous. It is easily seen that any rotation of  $\bar{\mathbf{c}}$ , say  $\bar{\mathbf{c}}e^{j\phi}$ ,  $\phi \in [0, 2\pi)$ , is optimal for EQP (this observation is always true for quadratically constrained quadratic optimization with homogeneous objective and constraint functions). Denoting by  $\phi = \arg(\bar{\mathbf{c}}^\dagger \mathbf{c}_0)$ , we claim that  $\bar{\mathbf{c}}e^{j\phi}$  is optimal for QP. To this end, we first observe that  $\Re((\bar{\mathbf{c}}e^{j\phi})^\dagger \mathbf{c}_0) = (\bar{\mathbf{c}}e^{j\phi})^\dagger \mathbf{c}_0 = |\bar{\mathbf{c}}^\dagger \mathbf{c}_0| \geq \sqrt{\delta_\epsilon} \geq 1 - \epsilon/2$ , thus  $\bar{\mathbf{c}}e^{j\phi}$  is a feasible solution of QP. Second, we note that the feasibility region of EQP is larger than that of QP; accordingly, the optimal value of EQP is greater than or equal to the optimal value of QP. Since we have found a feasible solution  $\bar{\mathbf{c}}e^{j\phi}$  of QP, which has the objective function value equal to the optimal value of EQP, hence  $\bar{\mathbf{c}}e^{j\arg(\bar{\mathbf{c}}^\dagger \mathbf{c}_0)}$  is optimal for QP.

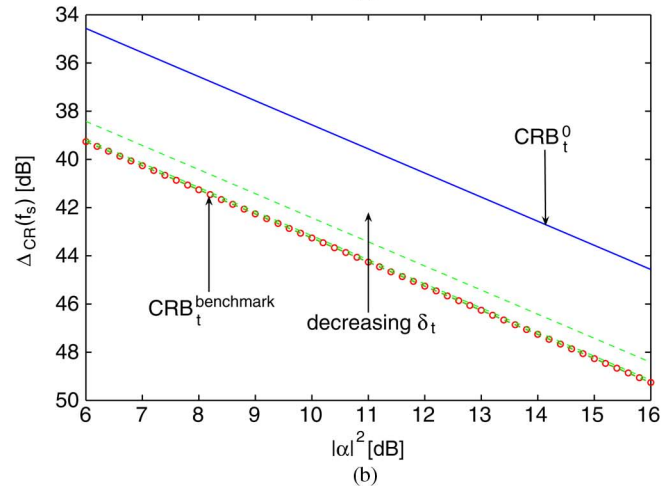
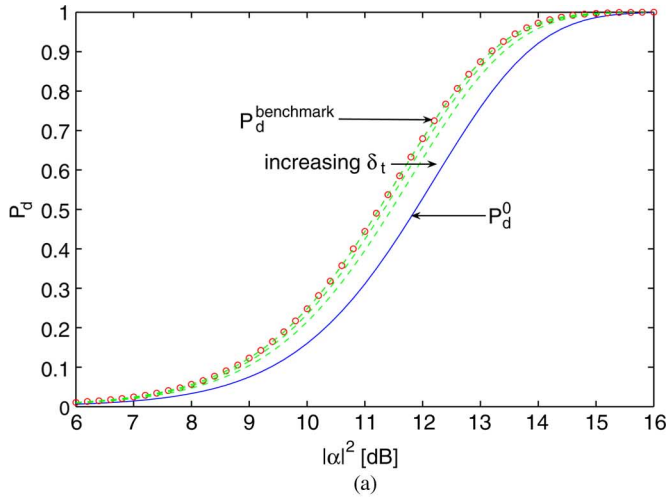


Fig. 9. (a)  $P_d$  versus  $|\alpha|^2$  for nonfluctuating target, real data,  $P_{fa} = 10^{-6}$ ,  $f_t = 0.25$ ,  $f_s = 0.15$ ,  $\delta_s = 30.6$ ,  $\delta_\epsilon = 0.001$ , and several values of  $\delta_t \in \{873.3, 1036.0, 1059.5\}$ . Generalized Barker code (solid curve).  $P_d$  of the proposed code for a given  $\delta_t$  (dashed curves). Benchmark  $P_d$  (o-marked dashed curve). (b)  $\Delta_{CR}(f_s)$  versus  $|\alpha|^2$  for nonfluctuating target, real data,  $f_t = 0.25$ ,  $f_s = 0.15$ ,  $\delta_s = 30.6$ ,  $\delta_\epsilon = 0.001$ , and several values of  $\delta_t \in \{873.3, 1036.0, 1059.5\}$ . Generalized Barker code (solid curve).  $\Delta_{CR}(f_s)$  of the proposed code for a given  $\delta_t$  (dashed curves). Benchmark  $\Delta_{CR}(f_s)$  (o-marked dashed curve).

### C. Strict Feasibility of REQP and REQPD

The strict feasibility of REQP is due to the assumption that QP is strictly feasible. In fact, suppose that there is  $\mathbf{c}_1$  such that  $\|\mathbf{c}_1\| = 1$ ,  $\mathbf{c}_1^\dagger \mathbf{R}_t \mathbf{c}_1 > \delta_t$ ,  $\mathbf{c}_1^\dagger \mathbf{R}_s \mathbf{c}_1 > \delta_s$ , and  $\Re(\mathbf{c}_1^\dagger \mathbf{c}_0) > 1 - \epsilon/2$ . Evidently,  $\mathbf{c}_1$  is also a strictly feasible solution of EQP. Now, we further assert that for sufficiently small  $\lambda > 0$ ,

$$\mathbf{C}_\lambda = (1 - \lambda)\mathbf{c}_1\mathbf{c}_1^\dagger + \frac{\lambda}{N}\mathbf{I},$$

is strictly feasible to REQP. Indeed,  $\mathbf{C}_\lambda$  is positive definite, and  $\text{tr}(\mathbf{C}_\lambda) = 1$ , for any  $1 \geq \lambda > 0$ . Moreover, for sufficiently small  $\lambda > 0$ , we have  $\text{tr}(\mathbf{C}_\lambda \mathbf{R}_t) = (1 - \lambda)\mathbf{c}_1^\dagger \mathbf{R}_t \mathbf{c}_1 + (\lambda/N)\text{tr}(\mathbf{R}_t) > \delta_t$ ,  $\text{tr}(\mathbf{C}_\lambda \mathbf{R}_s) = (1 - \lambda)\mathbf{c}_1^\dagger \mathbf{R}_s \mathbf{c}_1 + (\lambda/N)\text{tr}(\mathbf{R}_s) > \delta_s$ ,  $\text{tr}(\mathbf{C}_\lambda \mathbf{C}_0) = (1 - \lambda)\mathbf{c}_1^\dagger \mathbf{C}_0 \mathbf{c}_1 + (\lambda/N)\text{tr}(\mathbf{C}_0) > \delta_\epsilon$ . The strict feasibility of REQPD is immediate by setting  $y_1$  to be any number greater than the largest eigenvalue of  $\mathbf{R} + y_2 \mathbf{R}_t + y_3 \mathbf{R}_s + y_4 \mathbf{C}_0$  for given  $y_2 > 0$ ,  $y_3 > 0$ , and  $y_4 > 0$ .

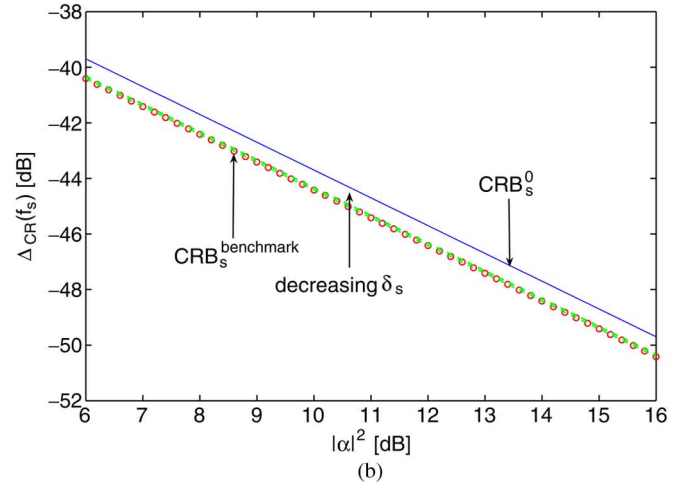
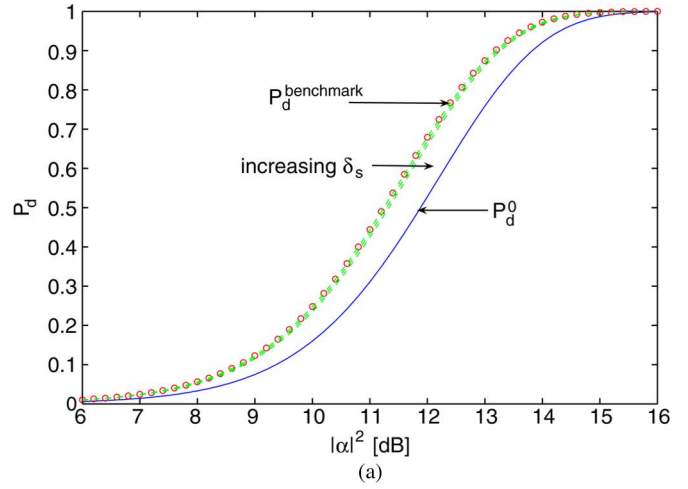


Fig. 10.  $P_d$  versus  $|\alpha|^2$  for nonfluctuating target, real data,  $f_t = 0.25$ ,  $f_s = 0.15$ ,  $\delta_t = 1.1$ ,  $\delta_\epsilon = 0.001$ , and several values of  $\delta_s \in \{29.3, 1351.6, 1381.7\}$ . Generalized Barker code (solid curve).  $P_d$  of the proposed code for a given  $\delta_s$  (dashed curves). Benchmark  $P_d$  (o-marked dashed curve). (b)  $\Delta_{CR}(f_s)$  versus  $|\alpha|^2$  for nonfluctuating target, real data,  $f_t = 0.25$ ,  $f_s = 0.15$ ,  $\delta_t = 1.1$ ,  $\delta_\epsilon = 0.001$ , and several values of  $\delta_s \in \{29.3, 1351.6, 1381.7\}$ . Generalized Barker code (solid curve).  $\Delta_{CR}(f_s)$  of the proposed code for a given  $\delta_s$  (dashed curves). Benchmark  $\Delta_{CR}(f_s)$  (o-marked dashed curve).

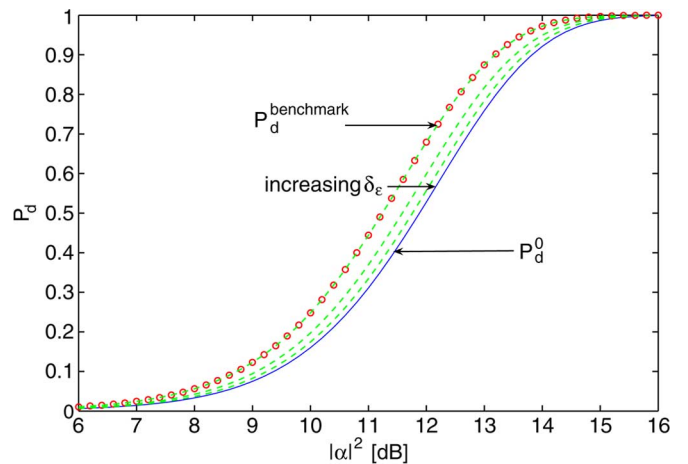


Fig. 11.  $P_d$  versus  $|\alpha|^2$  for nonfluctuating target, real data,  $P_{fa} = 10^{-6}$ ,  $f_t = 0.25$ ,  $f_s = 0.15$ ,  $\delta_t = 1.1$ ,  $\delta_s = 30.6$ , and several values of  $\delta_\epsilon \in \{0, 0.9792, 0.9974\}$ . Generalized Barker code (solid curve).  $P_d$  of the proposed code for a given  $\delta_\epsilon$  (dashed curves). Benchmark  $P_d$  (o-marked dashed curve).

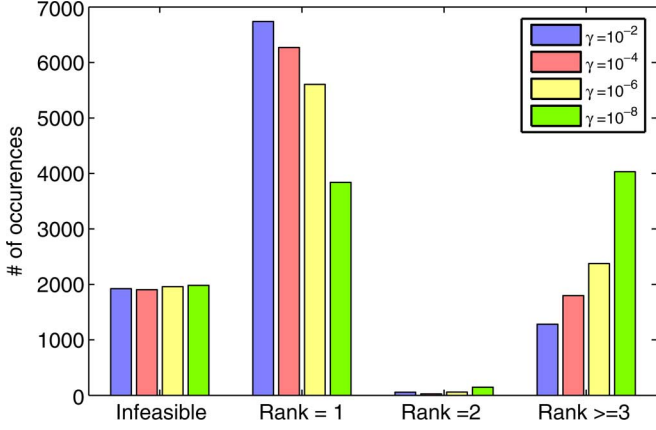


Fig. 12. Rank $_{\gamma}(\bar{\mathbf{C}})$ , over 10000 random experiments, for different values of  $\gamma \in \{10^{-2}, 10^{-4}, 10^{-6}, 10^{-8}\}$ .

#### D. Proof of Theorem I

*Proof:* The quadruple  $(\text{tr}(\mathbf{Y}), \text{tr}(\mathbf{Y}\mathbf{R}_t), \text{tr}(\mathbf{Y}\mathbf{R}_s), \text{tr}(\mathbf{Y}\mathbf{C}_0))$  is always  $\neq (0, 0, 0, 0)$ , since  $\text{tr}(\mathbf{Y}) \neq 0$  for any nonzero  $\mathbf{Y} \succeq 0$ . Thus, we can exploit Proposition II. The vector  $\bar{\mathbf{c}} = \mathcal{D}_4(\bar{\mathbf{C}}, \mathbf{I}, \mathbf{R}_t, \mathbf{R}_s, \mathbf{C}_0)$  complies with

$$\begin{aligned} \text{tr}(\bar{\mathbf{c}}\bar{\mathbf{c}}^\dagger) &= \text{tr}(\bar{\mathbf{C}}) = 1 \\ \text{tr}(\bar{\mathbf{c}}\bar{\mathbf{c}}^\dagger \mathbf{R}_t) &= \text{tr}(\bar{\mathbf{C}}\mathbf{R}_t) \geq \delta_t \\ \text{tr}(\bar{\mathbf{c}}\bar{\mathbf{c}}^\dagger \mathbf{R}_s) &= \text{tr}(\bar{\mathbf{C}}\mathbf{R}_s) \geq \delta_s \\ \text{tr}(\bar{\mathbf{c}}\bar{\mathbf{c}}^\dagger \mathbf{C}_0) &= \text{tr}(\bar{\mathbf{C}}\mathbf{C}_0) \geq \delta_\epsilon \\ \bar{\mathbf{c}}\bar{\mathbf{c}}^\dagger &\succeq \mathbf{0}. \end{aligned} \quad (28)$$

This implies that  $\mathbf{C}_{\text{opt}} = \bar{\mathbf{c}}\bar{\mathbf{c}}^\dagger$  is feasible to (13). Now, we check that  $\mathbf{C}_{\text{opt}} = \bar{\mathbf{c}}\bar{\mathbf{c}}^\dagger$  satisfies the optimality conditions (15)–(18) as well. To see this, we observe that  $\bar{\mathbf{c}} \in \text{range}(\bar{\mathbf{C}})$ , which means that there is  $\mathbf{z}$  such that  $\bar{\mathbf{c}} = \bar{\mathbf{C}}\mathbf{z}$ .

We claim that  $\mathbf{C}_{\text{opt}} = \bar{\mathbf{c}}\bar{\mathbf{c}}^\dagger$  satisfies the first optimality condition (15). Indeed,

$$\begin{aligned} &\text{tr}[(\bar{y}_1\mathbf{I} - \bar{y}_2\mathbf{R}_t - \bar{y}_3\mathbf{R}_s - \bar{y}_4\mathbf{C}_0 - \mathbf{R})\bar{\mathbf{C}}] = 0 \\ \Rightarrow &(\bar{y}_1\mathbf{I} - \bar{y}_2\mathbf{R}_t - \bar{y}_3\mathbf{R}_s - \bar{y}_4\mathbf{C}_0 - \mathbf{R})\bar{\mathbf{C}} = 0 \\ \Rightarrow &\mathbf{z}^\dagger \bar{\mathbf{C}}(\bar{y}_1\mathbf{I} - \bar{y}_2\mathbf{R}_t - \bar{y}_3\mathbf{R}_s - \bar{y}_4\mathbf{C}_0 - \mathbf{R})\bar{\mathbf{C}}\mathbf{z} = 0 \\ \Rightarrow &\bar{\mathbf{c}}^\dagger(\bar{y}_1\mathbf{I} - \bar{y}_2\mathbf{R}_t - \bar{y}_3\mathbf{R}_s - \bar{y}_4\mathbf{C}_0 - \mathbf{R})\bar{\mathbf{c}} = 0 \\ \Rightarrow &\text{tr}[(\bar{y}_1\mathbf{I} - \bar{y}_2\mathbf{R}_t - \bar{y}_3\mathbf{R}_s - \bar{y}_4\mathbf{C}_0 - \mathbf{R})\bar{\mathbf{c}}\bar{\mathbf{c}}^\dagger] = 0. \end{aligned}$$

Moreover,  $\mathbf{C}_{\text{opt}} = \bar{\mathbf{c}}\bar{\mathbf{c}}^\dagger$  complies with the optimality conditions (16)–(18), since

$$(\text{tr}(\bar{\mathbf{c}}\bar{\mathbf{c}}^\dagger \mathbf{R}_t) - \delta_t) \bar{y}_2 = (\text{tr}(\bar{\mathbf{C}}\mathbf{R}_t) - \delta_t) \bar{y}_2 = 0,$$

and

$$(\text{tr}(\bar{\mathbf{c}}\bar{\mathbf{c}}^\dagger \mathbf{R}_s) - \delta_s) \bar{y}_3 = (\text{tr}(\bar{\mathbf{C}}\mathbf{R}_s) - \delta_s) \bar{y}_3 = 0,$$

and

$$(\text{tr}(\bar{\mathbf{c}}\bar{\mathbf{c}}^\dagger \mathbf{C}_0) - \delta_\epsilon) \bar{y}_4 = (\text{tr}(\bar{\mathbf{C}}\mathbf{C}_0) - \delta_\epsilon) \bar{y}_4 = 0.$$

Therefore,  $\mathbf{C}_{\text{opt}} = \bar{\mathbf{c}}\bar{\mathbf{c}}^\dagger$  is an optimal solution of (13).

#### E. Proof of Theorem II

*Proof:* Suppose that  $\delta_4 > \delta_\epsilon$ , without loss of generality, because discussion for either the case  $\delta_2 > \delta_t$  or the case  $\delta_3 > \delta_s$  is similar. Then,  $\bar{y}_4 = 0$ ,  $\text{tr}(\bar{\mathbf{C}}(\delta_2\mathbf{I} - \mathbf{R}_t)) = 0$ , and  $\text{tr}(\bar{\mathbf{C}}(\delta_3\mathbf{I} - \mathbf{R}_s)) = 0$ . By Proposition I, there is a rank-one decomposition of  $\bar{\mathbf{C}} = \mathbf{c}_1\mathbf{c}_1^\dagger + \mathbf{c}_2\mathbf{c}_2^\dagger$  such that

$$\text{tr}[\mathbf{c}_i\mathbf{c}_i^\dagger(\delta_2\mathbf{I} - \mathbf{R}_t)] = 0, \quad \text{tr}[\mathbf{c}_i\mathbf{c}_i^\dagger(\delta_3\mathbf{I} - \mathbf{R}_s)] = 0, \quad i = 1, 2,$$

or equivalently,

$$\text{tr}\left(\mathbf{R}_t \frac{\mathbf{c}_i\mathbf{c}_i^\dagger}{\|\mathbf{c}_i\|^2}\right) = \delta_2, \quad \text{tr}\left(\mathbf{R}_s \frac{\mathbf{c}_i\mathbf{c}_i^\dagger}{\|\mathbf{c}_i\|^2}\right) = \delta_3, \quad i = 1, 2.$$

Let  $a_1 = \text{tr}(\bar{\mathbf{C}}\mathbf{c}_1\mathbf{c}_1^\dagger)$  and  $a_2 = \text{tr}(\bar{\mathbf{C}}\mathbf{c}_2\mathbf{c}_2^\dagger)$ . Then,  $\delta_4 = a_1 + a_2$ . Since  $\text{tr}(\mathbf{c}_1\mathbf{c}_1^\dagger + \mathbf{c}_2\mathbf{c}_2^\dagger) = 1$ , then  $0 < \|\mathbf{c}_1\| < 1$ ,  $0 < \|\mathbf{c}_2\| < 1$ , and  $0 \leq a_1 \leq \delta_4$ .

We claim that at least one of  $(\mathbf{c}_1^\dagger \bar{\mathbf{C}}\mathbf{c}_1 / \|\mathbf{c}_1\|^2) > \delta_\epsilon$  and  $(\mathbf{c}_2^\dagger \bar{\mathbf{C}}\mathbf{c}_2 / \|\mathbf{c}_2\|^2) > \delta_\epsilon$  is true. In fact, assume, *ab absurdo*, that

$$\frac{a_1}{\|\mathbf{c}_1\|^2} \leq \delta_\epsilon, \quad \frac{a_2}{\|\mathbf{c}_2\|^2} = \frac{\delta_4 - a_1}{1 - \|\mathbf{c}_1\|^2} \leq \delta_\epsilon.$$

This implies  $\delta_4 \leq \delta_\epsilon$ , which is in contrast with the assumption  $\delta_4 > \delta_\epsilon$ . Now, pick up the one between  $\mathbf{c}_1$  and  $\mathbf{c}_2$  which satisfies  $(\mathbf{c}_i^\dagger \bar{\mathbf{C}}\mathbf{c}_i / \|\mathbf{c}_i\|^2) > \delta_\epsilon$ ,  $i \in \{1, 2\}$ , say  $\mathbf{c}_1$ . It is easily seen that  $\mathbf{c}_1\mathbf{c}_1^\dagger / \|\mathbf{c}_1\|^2$  is feasible to REQP and satisfies the optimality conditions (15)–(18), namely it is an optimal solution of REQP.

#### REFERENCES

- [1] A. Farina, "Waveform diversity: Past, present, and future," presented at the 3rd Int. Waveform Diversity & Design Conf., Pisa, Jun. 2007, Plenary Talk.
- [2] A. Nehorai, F. Gini, M. S. Greco, A. Papandreou-Suppappola, and M. Rangaswamy, "Adaptive waveform design for agile sensing and communications," *IEEE J. Sel. Topics Signal Process. (Special Issue on Adaptive Waveform Design for Agile Sensing and Communications)*, vol. 1, no. 1, pp. 2–213, Jun. 2007.
- [3] P. A. Antonik, H. Griffith, D. D. Wiener, and M. C. Wicks, "Novel diverse waveform," Air Force Research Lab., New York, In-House Rep., Jun. 2001.
- [4] C. H. Wilcox, "The synthesis problem for radar ambiguity functions," Math Res. Center, U.S. Army, Univ. Wisconsin, Madison, WI, MRC Tech. Summary Rep. 157, Apr. 1960.
- [5] M. R. Bell, "Information theory and radar waveform design," *IEEE Trans. Inf. Theory*, vol. 39, no. 5, pp. 1578–1597, Sep. 1993.
- [6] A. Farina and F. A. Studer, "Detection with high resolution radar: Great promise, big challenge," *Microwave J.*, pp. 263–273, May 1991.
- [7] S. U. Pillai, H. S. Oh, D. C. Youla, and J. R. Guerci, "Optimum transmit-receiver design in the presence of signal-dependent interference and channel noise," *IEEE Trans. Inf. Theory*, vol. 46, no. 2, pp. 577–584, Mar. 2000.
- [8] D. A. Garren, A. C. Odom, M. K. Osborn, J. S. Goldstein, S. U. Pillai, and J. R. Guerci, "Full-polarization matched-illumination for target detection and identification," *IEEE Trans. Aerosp. Electron. Syst.*, vol. 38, no. 3, pp. 824–837, Jul. 2002.
- [9] S. Kay, "Optimal signal design for detection of point targets in stationary Gaussian clutter/reverberation," *IEEE J. Sel. Topics Signal Process.*, vol. 1, no. 1, pp. 31–41, Jun. 2007.
- [10] J. S. Bergin, P. M. Techau, J. E. Don Carlos, and J. R. Guerci, "Radar waveform optimization for colored noise mitigation," in *Proc. IEEE Inter. Radar Conf.*, Alexandria, VA, May 9–12, 2005, pp. 149–154.
- [11] J. Li, J. R. Guerci, and L. Xu, "Signal waveform's optimal-under-restriction design for active sensing," *IEEE Signal Process. Lett.*, vol. 13, no. 9, pp. 565–568, Sep. 2006.
- [12] N. Levanon and E. Mozeson, *Radar Signals*. New York: Wiley, 2004.

- [13] M. Bell, "Information theory of radar and sonar waveforms," in *Wiley Encyclopedia of Electrical and Electronic Engineering*, J. G. Webster, Ed. New York: Wiley-Interscience, 1999, vol. 10, pp. 180–190.
- [14] A. Leshem, O. Naparstek, and A. Nehorai, "Information theoretic adaptive radar waveform design for multiple extended targets," *IEEE J. Sel. Topics Signal Process.*, vol. 1, no. 1, pp. 42–55, Jun. 2007.
- [15] A. De Maio, S. De Nicola, Y. Huang, S. Zhang, and A. Farina, "Code design to optimize radar detection performance under accuracy and similarity constraints," *IEEE Trans. Signal Process.*, vol. 56, no. 11, pp. 5618–5629, Nov. 2008.
- [16] S. Boyd and L. Vandenberghe, *Convex Optimization*. Cambridge, U.K.: Cambridge Univ. Press, 2003.
- [17] A. Nemirovski, "Lectures on modern convex optimization," Georgia Instit. of Technology, Atlanta, GA, Fall, 2005, class notes.
- [18] A. De Maio, S. De Nicola, Y. Huang, Z.-Q. Luo, and S. Zhang, "Design of phase codes for radar performance optimization with a similarity constraint," *IEEE Trans. Signal Process.*, vol. 57, no. 2, pp. 610–621, Feb. 2009.
- [19] A. d'Aspermont and S. Boyd, "Relaxations and randomized methods for nonconvex QCQPs," Stanford Univ., Stanford, CA, Autumn, 2003, EE392o class notes.
- [20] W.-K. Ma, T. N. Davidson, K. M. Wong, Z.-Q. Luo, and P.-C. Ching, "Quasi-maximum-likelihood multiuser detection using semi-definite relaxation with application to synchronous CDMA," *IEEE Trans. Signal Process.*, vol. 50, no. 4, pp. 912–922, Apr. 2002.
- [21] A. Mobasher, M. Taherzadeh, R. Sotirov, and A. K. Khandani, "A near-maximum-likelihood decoding algorithm for MIMO systems based on semi-definite programming," *IEEE Trans. Inf. Theory*, vol. 53, no. 11, pp. 3869–3886, Nov. 2007.
- [22] E. Karipidis, N. D. Sidiropoulos, and Z.-Q. Luo, "Quality of service and max-min fair transmit beamforming to multiple cochannel multicast groups," *IEEE Trans. Signal Process.*, vol. 56, no. 3, pp. 1268–1279, Mar. 2008.
- [23] J. Ward, "Space-time adaptive processing for airborne radar," Lincoln Labs., MIT, Lexington, MA, Tech. Rep. 1015, Dec. 1994.
- [24] R. Klemm, *Principles of Space-Time Adaptive Processing*. London, U.K.: IEE Press, 2002.
- [25] J. R. Guerci, *Space-Time Adaptive Processing for Radar*. Norwood, MA: Artech House, 2003.
- [26] Y. Huang and S. Zhang, "Complex matrix decomposition and quadratic programming," *Math. Oper. Res.*, vol. 32, no. 3, pp. 758–768, Aug. 2007.
- [27] W. Ai, Y. Huang, and S. Zhang, "Further results on rank-one matrix decomposition and its applications," *Math. Programm.*, Jan. 2008, accepted for publication.
- [28] J. S. Bergin and P. M. Techau, "High-fidelity site-specific radar simulation: KASSPER '02 workshop datacube," in *ISL Technical Note, ISL-SCRD-TR-02-105*, Vienna, VA, May 2002.
- [29] R. A. Horn and C. R. Johnson, *Matrix Analysis*. Cambridge, U.K.: Cambridge Univ. Press, 1985.
- [30] H. L. Van Trees, *Optimum Array Processing. Part IV of Detection, Estimation and Modulation Theory*. New York: Wiley, 2002.
- [31] P. Antonik, M. C. Wicks, H. D. Griffiths, and C. J. Baker, "Frequency diverse array radars," in *Proc. 2006 IEEE Int. Radar Conf.*, Verona, NY, Apr. 24–27, 2006, pp. 215–217.
- [32] P. Antonik, M. C. Wicks, H. D. Griffiths, and C. J. Baker, "Multi-mission multi-mode waveform diversity," in *Proc. 2006 IEEE Int. Radar Conf.*, Verona, NY, Apr. 24–27, 2006, pp. 580–582.
- [33] J. S. Goldstein, I. S. Reed, and P. A. Zulch, "Multistage partially adaptive STAP CFAR detection algorithm," *IEEE Trans. Aerosp. Electron. Syst.*, vol. 35, no. 2, pp. 645–661, Apr. 1999.
- [34] L. Bomer and M. Antweiler, "Polyphase Barker sequences," *Electron. Lett.*, vol. 25, no. 23, pp. 1577–1579, Nov. 1989.
- [35] M. Friese, "Polyphase Barker sequences up to length 36," *IEEE Trans. Inf. Theory*, vol. 42, no. 4, pp. 1248–1250, Jul. 1996.
- [36] J. F. Sturm, "Using SeDuMi 1.02, a MATLAB toolbox for optimization over symmetric cones," *Optim. Methods Softw.*, vol. 11–12, pp. 625–653, Aug. 1999.
- [37] E. Mozeson and N. Levanon, "MATLAB code for plotting ambiguity functions," *IEEE Trans. Aerosp. Electron. Syst.*, vol. 38, no. 3, pp. 1064–1068, Jul. 2002.
- [38] A. De Maio and M. Lops, "Design principles of MIMO radar detectors," *IEEE Trans. Aerosp. Electron. Syst.*, vol. 43, no. 3, pp. 886–898, Jul. 2007.
- [39] Y. Yang and R. S. Blum, "Minimax robust MIMO radar waveform design," *IEEE J. Sel. Topics Signal Process.*, vol. 1, no. 1, pp. 42–55, Jun. 2007.

- [40] J. Li and P. Stoica, *MIMO Radar Signal Processing*. New York: Wiley, 2009.
- [41] R. E. Blahut, W. M. Miller, and C. H. Wilcox, *Radar and Sonar*. New York: Springer-Verlag, 1991, pt. 1, reprint.



**Antonio De Maio** (S'01–AM'02–M'03–SM'07) was born in Sorrento, Italy, on June 20, 1974. He received the Dr.Eng. degree (with honors) and the Ph.D. degree in information engineering, both from the University of Naples Federico II, Naples, Italy, in 1998 and 2002, respectively.

From October to December 2004, he was a visiting researcher at the U.S. Air Force Research Laboratory, Rome, NY. From November to December 2007, he was a visiting researcher at the Chinese University of Hong Kong, Hong Kong. Currently, he is an Associate Professor at the University of Naples Federico II. His research interest lies in the field of statistical signal processing, with emphasis on radar detection, convex optimization applied to radar signal processing, and multiple-access communications.



**Silvio De Nicola** (S'07) received the Dr. Eng. degree (*summa cum laude*) in telecommunication engineering from the University of Naples Federico II, Italy, in 2004. He is currently working towards the Ph.D. degree in information and telecommunication engineering at the Department of Electronic and Telecommunication Engineering in the same university.

Until 2006, he worked as consultant in Telecom Italy. In 2007, he was a visiting student at the Chinese University of Hong Kong. He works for the Italian regulatory authority in the communications sector (AGCOM). His research interest lies in optimization theory, with emphasis on radar signal processing.



**Yongwei Huang** (M'09) received the B.Sc. degree in computational mathematics and M.Sc. degree in operations research, both from Chongqing University, in 1998 and 2000, respectively, and the Ph.D. degree in operations research from the Chinese University of Hong Kong in 2005.

He was a Postdoctoral Fellow at the Department of Systems Engineering and Engineering Management, the Chinese University of Hong Kong, and a visiting researcher of the Department of Biomedical, Electronic, and Telecommunication Engineering at the University of Napoli "Federico II," Italy. Currently, he is a Research Associate at the Department of Electronic and Computer Engineering, the Hong Kong University of Science and Technology. His research interests are related to optimization theory and algorithms, including conic optimization, robust optimization, combinatorial optimization, and stochastic optimization, and their applications in signal processing, radar, and wireless communications.



**Daniel P. Palomar** (S'99–M'03–SM'08) received the Electrical Engineering and Ph.D. degrees (both with honors) from the Technical University of Catalonia (UPC), Barcelona, Spain, in 1998 and 2003, respectively.

Since 2006, he has been an Assistant Professor in the Department of Electronic and Computer Engineering at the Hong Kong University of Science and Technology (HKUST), Hong Kong. He has held several research appointments, namely, at King's College London (KCL), London, U.K.; Technical University of Catalonia (UPC), Barcelona, Spain; Stanford University, Stanford, CA; Telecommunications Technological Center of Catalonia (CTTC), Barcelona, Spain; Royal Institute of Technology (KTH), Stockholm, Sweden; University of Rome "La Sapienza," Rome, Italy; and Princeton University, Princeton, NJ. His current research interests include applications of convex

optimization theory, game theory, and variational inequality theory to signal processing and communications.

Dr. Palomar is an Associate Editor of the IEEE TRANSACTIONS ON SIGNAL PROCESSING, a Guest Editor of the IEEE SIGNAL PROCESSING MAGAZINE 2010 Special Issue on Convex Optimization for Signal Processing, was a Guest Editor of the IEEE JOURNAL ON SELECTED AREAS IN COMMUNICATIONS 2008 Special Issue on Game Theory in Communication Systems, as well as the Lead Guest Editor of the IEEE JOURNAL ON SELECTED AREAS IN COMMUNICATIONS 2007 Special Issue on Optimization of MIMO Transceivers for Realistic Communication Networks. He serves on the IEEE Signal Processing Society Technical Committee on Signal Processing for Communications (SPCOM). He is a recipient of a 2004/2006 Fulbright Research Fellowship; the 2004 Young Author Best Paper Award by the IEEE Signal Processing Society; the 2002/2003 best Ph.D. prize in Information Technologies and Communications by the Technical University of Catalonia (UPC); the 2002/2003 Rosina Ribalta first prize for the Best Doctoral Thesis in Information Technologies and Communications by the Epson Foundation; and the 2004 prize for the Best Doctoral Thesis in Advanced Mobile Communications by the Vodafone Foundation and COIT.



**Shuzhong Zhang** received the B.Sc. degree in applied mathematics from Fudan University in 1984 and the Ph.D. degree in operations research and econometrics from the Tinbergen Institute, Erasmus University, in 1991.

He is a Professor at the Department of Systems Engineering and Engineering Management at The Chinese University of Hong Kong. He had held faculty positions in Department of Econometrics, University of Groningen, from 1991 to 1993, and the Econometric Institute, Erasmus University, from 1993 to

1999. Since 1999, he has been with the Department of Systems Engineering and Engineering Management, The Chinese University of Hong Kong. His current research interests include conic, robust, and stochastic optimization.

Dr. Zhang received the Erasmus University Research Prize in 1999, the CUHK Vice-Chancellor Exemplary Teaching Award in 2001, and the SIAM Outstanding Paper Prize in 2003. He is an elected Council Member at Large of the MPS (Mathematical Programming Society) from 2006 to 2009, and is Vice-President of the Operations Research Society of China (since 2008). He serves on the Editorial Board of six academic journals, including *Operations Research*, and *SIAM Journal on Optimization*.



**Alfonso Farina** (M'95–SM'98–F'00) received the Ph.D. degree in electronic engineering from the University of Rome (I), Italy, in 1973.

In 1974, he joined Selenia, now SELEX-Sistemi Integrati, where he has been a Manager since May 1988. He was Scientific Director in the Chief Technical Office. Currently, he is Director of the Analysis of Integrated Systems Unit. In his professional life, he has provided technical contributions to detection, signal, data, image processing, and fusion for the main radar systems conceived, designed, and developed in the Company.

He has provided leadership in many projects—also conducted in the international arena—in surveillance for ground and naval applications, in airborne early warning and in imaging radar. From 1979 to 1985, he has also been Professor of radar techniques at the University of Naples; in 1985, he was appointed Associate Professor. He is the author of more than 500 peer-reviewed technical publications and the author of books and monographs: *Radar Data Processing*, Vols. 1 and 2, translated in Russian and Chinese, (Researches Studies Press (U.K.), Wiley (U.S.), 1985–1986); *Optimized Radar Processors*, (London, U.K., IEE/Peregrinus, 1987); and *Antenna Based Signal Processing Techniques for Radar Systems* (Norwood, MA: Artech House, 1992). He wrote the chapter “ECCM Techniques” in the *Radar Handbook* (New York: McGraw-Hill, 2nd ed., 1990, and 3rd ed., 2008), edited by Dr. M. I. Skolnik.

Dr. Farina has been session chairman at many international radar conferences. In addition to lecturing at universities and research centers in Italy and abroad, he also frequently gives tutorials at the International Radar Conferences on signal, data, and image processing for radar, in particular on multisensor fusion, adaptive signal processing, space-time adaptive processing (STAP), and detection. In the 1987, he received the Radar Systems Panel Award of IEEE Aerospace and Electronic Systems Society (AESS) for development of radar data processing techniques. He is the Italian representative at the International Radar Systems Panel of the IEEE AESS. He is the Italian industrial representative (Panel Member at Large) at the Sensor and Electronic Technology (SET) of the Research Technology Organisation (RTO) of NATO. He has served on the Board of Directors of the International Society for Information Fusion (ISIF). He has been the Executive Chair of the International Conference on Information Fusion (Fusion) 2006, Florence, Italy, July 10–13, 2006. He was nominated Fellow of IEEE with the following citation: “For development and application of adaptive signal processing methods for radar systems.” Recently, he has been nominated international fellow of the Royal Academy of Engineering, U.K.; this fellowship was presented to him by HRH Prince Philip, the Duke of Edinburgh. He is a referee of numerous publications submitted to several journals of the IEEE, IEE, Elsevier, etc. He has also cooperated with the Editorial Board of the IEE *Electronics & Communication Engineering Journal*. More recently, he has served as a member of the Editorial Board of *Signal Processing* (Elsevier) and has been Co-Guest Editor of its Special Issue on New Trends and Findings in Antenna Array Processing for Radar, September 2004. He is the corecipient of the best paper awards entitled to B. Carlton of the IEEE TRANSACTIONS ON AEROSPACE AND ELECTRONIC SYSTEMS for 2001 and 2003 and also of the International Conference on Fusion 2005. He has been the leader of the team that received the 2002 AMS CEO award for Innovation Technology. He has been the corecipient of the AMS Radar Division award for Innovation Technology in 2003. Moreover, he has been the corecipient of the 2004 AMS CEO award for Innovation Technology. He has been the leader of the team that won the 2004 First Prize Award for Innovation Technology of Finmeccanica, Italy. This award context has seen the submission of more than 320 projects. This award has been set for the first time in 2004. On September 7, 2006, he received the Annual European Group Technical Achievement Award 2006 by the European Association for Signal, Speech and Image Processing, with the citation: “For development and application of adaptive signal processing technique in practical radar systems.” In October 2006, he was on the team that received the annual Innovation Technology award of Selex-SI for “an emulator of an integrated system for border control surveillance.” He has been appointed a member of the Editorial Boards of *IET Radar, Sonar and Navigation and of Signal, Image, and Video Processing Journal* (SIVP). He has been the General Chairman of the IEEE Radar Conference 2008, Rome, May 26–30, 2008. He is the recipient of the 2010 IEEE Dennis J. Picard Medal for Radar Technologies and Applications with the following citation: “For continuous, innovative, theoretical and practical contributions to radar systems and adaptive signal processing techniques.”